PERGAMON

International Journal of Solids and Structures 37 (2000) 2059–2087

INTERNATIONAL JOURNAL OF SOLIDS and STRUCTURES

www.elsevier.com/locate/ijsolstr

The effect of finite primary deformations on harmonic waves in layered elastic media

Graham A. Rogerson*, Kevin J. Sandiford

Department of Computer and Mathematical Sciences, University of Salford, Salford M5 4WT, UK

Received 10 September 1998

Abstract

The problem of extensional wave propagation in a pre-stressed, incompressible, 4-ply symmetric layered structure is considered. The high wave number behaviour of the harmonics is shown to fall into one of four distinct cases. Each of these are examined in detail and appropriate asymptotic expansions, giving phase speed as a function of wave number, are obtained. These are shown to provide excellent agreement with the numerical solution. A surface wave front arising from the combined influence of all harmonics is observed numerically. Corresponding plots of the eigenfunctions confirm that this is indeed a surface wave with the behaviour associated with each harmonic remarkably sensitive to changes in wave number. This paper concludes with a comparison of extensional and flexural waves.

Keywords: Waves; Layered media; Pre-stress

1. Introduction

Primarily motivated by the increasing industrial application of laminated structures, theoretical study of wave motion and vibration in layered media has been an area of considerable research activity in recent years. In this paper we continue in the spirit of such studies and examine the effects of pre-stress on small amplitude waves in layered media. Although stress is often induced in the manufacturing process, by techniques such as fabrication, the type of scenario we envisage is one in which pre-stress arises through the action of external forces. Problems involving the effect of pre-stress on waves in bounded media was instigated initially in the context of surface waves by Hayes and Rivlin (1961) and Flavin (1963). Additionally, and in the context of single layer plates, the effects of pre-stress have been investigated recently by Ogden and Roxburgh (1993), Rogerson and Fu (1995).

* Corresponding author. Tel: 0044 0161 2953345; fax: 0044 0161 2955559.
E-mail address: g.a.rogerson@cms.salford.ac.uk (G.A. Rogerson).

0020-7683/00/$ - see front matter
PII: S0020-7683(98)00347-3

In this paper we specifically investigate the effect of pre-stress on small amplitude extensional waves in symmetric 4-ply incompressible, elastic laminated structures. This work is presented in respect of the most general appropriate strain energy function and as such will both generalise previous work, Rogerson and Sandiford (1996), and offer the corresponding analysis to a previously published work on flexural waves, see Rogerson and Sandiford (1997). The reader is referred to this latter paper for a detailed reference list to waves in pre-stressed media. The motivation is to give some detailed indications of the precise influence of pre-stress on material characteristics.

We begin this paper in Section 2 with a brief review of the basic equations and derivation of both the extensional and flexural dispersion relation. In Section 3 various numerical solutions of the dispersion relation associated with extensional waves are presented which specifically show phase speed against scaled wave number. It is established that four distinct cases exist which are associated with the moderate and high wave number regions and are classified in terms of material parameters. Additionally a surface wave front is observed in some of these numerical solutions to arise from the cumulative effect of harmonics. In Section 4 asymptotic high wave number expansions are derived for each of the four previously mentioned cases and are observed to provided excellent agreement with the numerical solution. It is envisaged that these expansions will aid investigation of impact problems, specifically in estimation of errors incurred in numerical truncation of wave number integrals. In Section 5 the surface-wave-like behaviour associated with the harmonics is explicated by examining the corresponding in-plane and out-plane eigenfunctions. The harmonics are clearly observed to show classic surface wave behaviour over a specific wave number region and rapidly transform to sinusoidal variation outside this wave number region. The paper is concluded in Section 6 with a numerical comparison of the dispersion relations associated with extensional and flexural waves.

2. Basic equations and the dispersion relation

In this section we briefly review the basic equations governing small amplitude, time dependent motions superimposed upon a large static primary deformation in respect of small amplitude travelling waves in an incompressible elastic layer. The appropriate dispersion relation associated with both flexural and extensional waves in a 4-ply symmetric laminate is then derived by satisfying continuity conditions across each perfectly bonded interface and utilising boundary conditions of zero incremental traction. For details concerning the derivation of the solutions represented here the reader is referred to Rogerson and Sandiford (1996), and for a more detailed examination of the basic equations see Dowaikh and Ogden (1990).

Consider a 4-ply laminated plate which is symmetrical about its mid-plane, consists of two identical outer layers of width h, an inner core of width $2d$ and is of infinite extent in each of the remaining spatial directions. The material of the inner core and the outer layers is that of a pre-stressed, incompressible elastic solid with principal axes of the right Cauchy–Green strain tensor assumed co-incident for each layer. An appropriate Cartesian coordinate system $Ox_1x_2x_3$ is chosen coincident with the principal axes in the pre-stressed equilibrium state, such that Ox_2 is normal to the plane of the plate, Ox_1 is the direction of propagation and the origin O is at the mid-plane of the structure. A plane strain simplification of the equations of motion associated with the outer layer yields the two non-trivial equations

$$B_{1111}u_{1,11} + (B_{1122} + B_{2112})u_{2,21} + B_{2121}u_{1,22} - p^*_{,1} = \rho\ddot{u}_1, \tag{2.1}$$

$$(B_{1221} + B_{2211})u_{1,12} + B_{1212}u_{2,11} + B_{2222}u_{2,22} - p^*_{,2} = \rho\ddot{u}_2, \tag{2.2}$$

in which it has been assumed $u_3 \equiv 0$ and u_1 and u_2 are independent of x_3. Furthermore, in eqns (2.1) and (2.2) B_{ijkl} are components of the appropriate fourth-order elasticity tensor, p^* is a time-dependent pressure increment, ρ the density of the material and a comma indicates differentiation with respect to the implied spatial co-ordinate component in the finitely deformed equilibrium state B_e. In addition, two non-zero linearised traction increments are obtainable in the component form

$$\tau_1 = B_{2121}u_{1,2} + (B_{2112} + \bar{p})u_{2,1}, \tag{2.3}$$

$$\tau_2 = B_{2211}u_{1,1} + (B_{2222} + \bar{p})u_{2,2} - p^*, \tag{2.4}$$

with $\bar{p}$ denoting a static pressure in B_e.

Solutions of the basic equations governing small amplitude motions for displacement and incremental traction in an incompressible layer, under the assumption of plane strain, may be specified using the so-called propagator matrix $\mathbf{P}$, thus

$$\mathbf{Y}(x_2) = \mathbf{P}(x_2 - \bar{x}_2)\mathbf{Y}(\bar{x}_2), \tag{2.5}$$

where $\mathbf{Y}(x_2)$ is a vector of displacement and traction defined as $\mathbf{Y}(x_2) = (-iU, V, \tau_1/ik, \tau_2/k)^{\mathrm{T}}$, $\boldsymbol{\tau}$ is the incremental traction and U and V are eigenfunctions of the superimposed motion $\mathbf{u}$ in the form of the travelling wave, namely $(u_1, u_2) = (U, V)\,\mathrm{e}^{kqx_2}\,\mathrm{e}^{ik(x_1 - vt)}$, with k being the wave number and v the phase speed. The components of the propagator matrix are given in the appendix and q is constrained in order to yield non-trivial solutions, thus

$$\gamma q^4 + (\rho v^2 - 2\beta)q^2 + \alpha - \rho v^2 = 0, \tag{2.6}$$

within which α, β and γ are material parameters defined in terms of the components of the fourth-order elasticity tensor B_{ijkl} by

$$\alpha = B_{1212}, \quad 2\beta = B_{1111} + B_{2222} - 2B_{1122} - 2B_{1221}, \quad \gamma = B_{2121.}$$

Denoting the two roots of eqn (2.6) by q_1^2 and q_2^2 it is noted for future reference that

$$\gamma(q_1^2 + q_2^2) = 2\beta - \rho v^2, \quad \gamma q_1^2 q_2^2 = \alpha - \rho v^2. \tag{2.7}$$

Eqn (2.5) therefore provides a relationship between the values of displacement and traction at an arbitrary location in a layer to the (unknown) values at some specific location $x_2 = \bar{x}_2$ via the propagator matrix. For specified values of the material parameters α, β, γ and ρ the propagator matrix is a function of wave number k, phase speed v and the distance $x_2 - \bar{x}_2 = h$, say. For more details concerning the properties of the propagator matrix see Gilbert and Backus (1966). It is reiterated that eqns (2.5)–(2.7) have been derived under a plane strain simplification, in that it is assumed that all time dependent quantities are independent of x_3 and that $u_3 \equiv 0$. This has the consequence of reducing the subsequent boundary and continuity conditions from a linear homogeneous system of six equations in six unknowns to a system of four equations in four unknowns.

The material parameters α, β, γ and ρ are used to represent the material of the outer two layers and eqn (2.5) is used to represent the associated solutions of displacement and traction. The corresponding parameters for the inner core are denoted by $\tilde{\alpha}$, $\tilde{\beta}$, $\tilde{\gamma}$ and $\tilde{\rho}$, and lead to different solutions of the governing equations. These different solutions are generally denoted by imposing an over tilde, and using p_m rather than q_m, thus the solutions for the inner core take the form

$$\tilde{\mathbf{Y}}(x_2) = \tilde{\mathbf{P}}(x_2 - \bar{x}_2)\tilde{\mathbf{Y}}(\bar{x}_2), \tag{2.8}$$

where $\tilde{\mathbf{Y}} = (-i\tilde{U}, \tilde{V}, \tilde{\tau}_1/ik, \tilde{\tau}_2/k)^{\mathrm{T}}$ and $\tilde{\mathbf{P}}$ is the appropriate propagator matrix, which may be deduced directly from $\mathbf{P}$ with appropriate notational changes. Continuity conditions across the upper interface may now be expressed in the form $\mathbf{Y}(d) = \tilde{\mathbf{Y}}(d)$. By using eqns (2.5) and (2.8) with the continuity condition it is possible to relate the solution at the upper most surface $x_2 = h + d$ in terms of the solutions at the upper-most interface $x_2 = d$ and then in terms of the solution at the mid-plane, thus

$$\mathbf{Y}(d+h) = \mathbf{P}(h)\tilde{\mathbf{P}}(d)\tilde{\mathbf{Y}}(0). \tag{2.9}$$

We first consider extensional waves for which $\tilde{V}$ and $\tilde{\tau}_1$ vanish at the mid-plane. Incorporating this condition with both the boundary condition of zero incremental traction on the upper surface and continuity across the perfectly bonded upper interface yields a system of four equations in four unknowns, which will yield a non-trivial solution provided

$$P_{3i}\tilde{P}_{i1}P_{4j}\tilde{P}_{j4} - P_{3i}\tilde{P}_{i4}P_{4j}\tilde{P}_{j1} = 0. \tag{2.10}$$

Eqn (2.10) is the dispersion relation for extensional waves in the symmetric 4-ply structure. For the corresponding derivation of the dispersion relation associated with flexural waves it is required that $\tilde{U}$ and $\tilde{\tau}_2$ vanish on the mid-plane, implying that

$$P_{3i}\tilde{P}_{i2}P_{4j}\tilde{P}_{j3} - P_{3i}\tilde{P}_{i3}P_{4j}\tilde{P}_{j2} = 0, \tag{2.11}$$

see Rogerson and Sandiford (1996). Throughout the greater part of this paper our concern is with extensional waves. The dispersion relation associated with flexural waves is quoted to facilitate later comparison of numerical results. Inserting the definitions of the appropriate components of the two propagator matrices, and on the removal of a common factor, eqn (2.10) may be stated explicitly as

$$\begin{aligned} 2q_1q_2f(q_1)f(q_2)\Delta_1 + q_1f(q_2)^2\{&-C_1S_2\Delta_2 + C_1C_2\Delta_3 + S_1S_2\Delta_4 - S_1C_2\Delta_5\} \\ &+ q_2f(q_1)^2\{S_1C_2\Delta_2 - S_1S_2\Delta_3 - C_1C_2\Delta_4 + C_1S_2\Delta_5\} = 0, \end{aligned} \tag{2.12}$$

where

$$\begin{aligned} \Delta_1 &= p_1q_2\{\tilde{f}(p_2) - f(q_2)\}\{f(q_1) - \tilde{f}(p_2)\}\tilde{C}_1\tilde{S}_2 + p_2q_2\{\tilde{f}(p_1) - f(q_2)\}\{\tilde{f}(p_1) - f(q_1)\}\tilde{S}_1\tilde{C}_2, \\ \Delta_2 &= p_1p_2\{f(q_2) - f(q_1)\}\tilde{f}(p_1) - \{\tilde{f}(p_2)\}\tilde{C}_1\tilde{C}_2, \\ \Delta_3 &= p_1q_2\{\tilde{f}(p_2) - f(q_1)\}^2\tilde{C}_1\tilde{S}_2 - p_2q_2\{\tilde{f}(p_1) - f(q_1)\}^2\tilde{S}_1\tilde{C}_2, \\ \Delta_4 &= p_2q_1\{\tilde{f}(p_1) - f(q_2)\}^2\tilde{S}_1\tilde{C}_2 - p_1q_1\{\tilde{f}(p_2) - f(q_2)\}^2\tilde{C}_1\tilde{S}_2, \\ \Delta_5 &= q_2q_2\{f(q_2) - f(q_1)\}\{\tilde{f}(p_1) - \tilde{f}(p_2)\}\tilde{S}_1\tilde{S}_2, \end{aligned}$$

within which

$$\begin{aligned} &f(q_m) = \gamma\left(1 + q_m^2\right) - \sigma_2, \quad \tilde{f}(p_m) = \tilde{\gamma}\left(1 + p_m^2\right) - \sigma_2, \\ &S_m = \sinh kq_mh, \quad \tilde{S}_m = \sinh kp_md, \\ &C_m = \cosh kq_mh, \quad \tilde{C}_m = \cosh kp_md, \end{aligned}$$

and σ_2 is the principal Cauchy stress along the Ox_2-direction.

It is noted that q_1 and q_2 (p_1 and p_2) may be either real, purely imaginary or complex conjugates. The implication is that there exists twenty five distinct cases to consider if one wishes to solve the dispersion

equation numerically. However, in each case the dispersion relation remains either real or purely imaginary. This is shown most easily by considering the components of the propagator matrices $\mathbf{P}(h)$ [and $\tilde{\mathbf{P}}(d)$] given in the Appendix. It is easily verified that all components of $\mathbf{P}(h)$ [and similarly $\tilde{\mathbf{P}}(d)$] remain real in the cases when one or both of q_1 and q_2 (p_1 and p_2) are purely imaginary. In the case when q_1 and q_2 (p_1 and p_2) are complex conjugates each component of $\mathbf{P}(h)$ [$\tilde{\mathbf{P}}(d)$] is a quotient formed by the difference of two complex conjugates, thus ensuring that the components of $\mathbf{P}(h)$ [$\tilde{\mathbf{P}}(d)$] all remains real in this case. It is also noted that the removal of a common factor from the dispersion relation (2.12) means that whilst all the components of each propagator matrix are always real, the dispersion relation as expressed in the form of eqn (2.12) will either be real or purely imaginary.

3. Numerical results for extensional waves

The results of a numerical investigation of the dispersion relation for extensional waves (2.12) are presented here. These numerical results relate to four specific materials, two associated with the Mooney–Rivlin strain energy and two with the Varga strain energy.

3.1. Mooney–Rivlin material

Two figures of dispersion curves will now be presented using material parameters for the inner core and outer layers generated from the Mooney–Rivlin strain energy function.

$$W = \mathscr{C}_1\left(\lambda_1^2+\lambda_2^2+\lambda_3^2-3\right)+\mathscr{C}_2\left(\lambda_1^2\lambda_2^2+\lambda_2^2\lambda_3^2+\lambda_1^2\lambda_3^2-3\right), \tag{3.1}$$

in which $\mathscr{C}_1$ and $\mathscr{C}_2$ are material constants and λ_1, λ_2 and λ_3 are principal stretches of the primary deformation. The two Mooney–Rivlin materials used in the inner core and outer layers are summarised, along with the corresponding values of α, β and γ, in Table 1.

In Fig. 1 a graph is presented which shows the phase speed against scaled wave number for the first twenty five branches of the dispersion relation (2.12) and is generated for a laminate formed from materials 1 and 2 (from Table 1) in the outer layers and inner core, respectively. For these material parameters the fundamental mode has a high wave number limit corresponding to a Rayleigh surface wave with speed $v_R = 1.1823$, associated with the outer layers, while the harmonics asymptote to a shear wave speed associated with the outer layers, denoted by v_{S_1} and termed the first shear wave speed of the outer layers. Numerically it is observed that as $kh, kd \to \infty$ one of q_1 and q_2 is imaginary, the other real, with p_1 and p_2 real. (A similar asymptotic structure occurs when p_1 and p_2 form a complex conjugate pair.) It is further inferred from numerical analysis that if $q_1 = i\hat{q}_1$, then $\hat{q}_1 \to 0$ as $kh, kd \to \infty$. The specific value of v_{S_1} is then found by putting $q = 0$ in eqn (2.6) and is therefore given by $\rho v_{S_1}^2 = \alpha$. A

Table 1
Mooney–Rivlin and Varga materials used in generating dispersion curves. Note $\lambda_3 = (\lambda_1\lambda_2)^{-1}$

Material	$\mathscr{C}_1$	$\mathscr{C}_2$	λ_1	λ_2	α	2β	γ
1	1.2	0.3	1.0	0.866	2.0	3.5	1.5
2	1.6	0.2	1.414	0.707	4.0	5.0	1.0
3	4.5	—	1.5	1.0	4.05	5.4	1.8
4	2.2	—	2.0	0.5	3.52	1.76	0.22

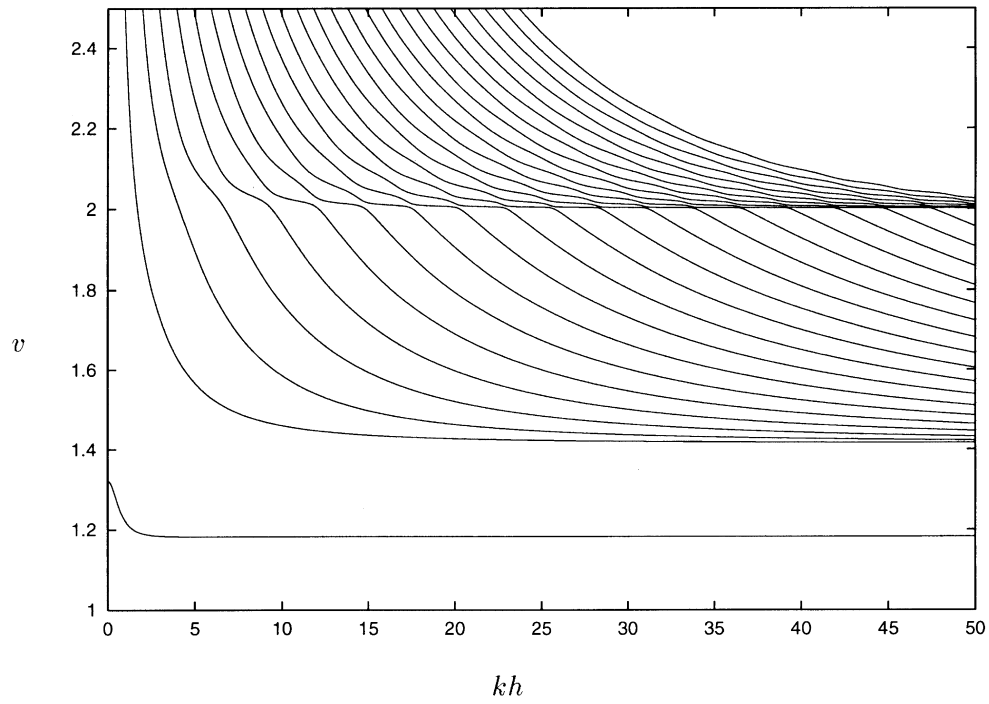

Fig. 1. Phase speed against scaled wave number for Mooney–Rivlin materials 1 and 2 from Table 1 in the outer layers and inner core, respectively, and $\sigma_2 = 2.5$, with $v_R = 1.1823$, no real v_I, $v_{S_1} = 1.414$, $\tilde{v}_{S_1} = 2.0$, no real v_{S_2} and $\tilde{v}_{S_2} = 1.732$.

further point to note from eqn (2.6) is that for q_2 to be real $\alpha \geqslant 2\beta$. This high wave number limit is to be referred to as Case 1. In the low wave number limit it is only the fundamental mode which retains finite wave speed. The flattening of the dispersion curves to form a ghost line is evident, this occurring at the first shear wave speed of the inner core $\tilde{v}_{S_1}$, obtained by putting $p = 0$ in the analogous appropriate form of (2.6) to yield $\tilde{\rho}\,\tilde{v}_{S_1}^2 = \tilde{\alpha}$.

The second plot, Fig. 2, is generated using materials 1 and 2 from Table 1 for the inner core and outer layers, respectively. The fundamental mode and all harmonics tend to $\tilde{v}_{S_1}$ in the high wave limit, a scenario termed Case 2. Numerically therefore, in this case only one of p_1 and p_2 is real, the other imaginary, with q_1 and q_2 being real (or complex conjugates) in the high wave limit. Accordingly it is deduced that if $p_1 = i\hat{p}_1$, then $|p_1| \to 0$ as $kh, kd \to \infty$ and $2\tilde{\beta} > \tilde{\alpha}$. For the material parameters and the value of σ_2 chosen there exists a surface wave speed greater than the limiting wave speed of all the harmonics. As previously discussed by Rogerson and Sandiford (1997), this is not a valid limit for the harmonics as $kh, kd \to \infty$ but rather causes flattening of the dispersion curves around the appropriate value of the surface wave speed v_R, forming a sharp line across the harmonics. Such a sharp flattening gives rise to surface-wave-like behaviour arising from the combined effect of the higher harmonics and will be discussed in more detail in a later section.

3.2. Varga material

A further set of two figures are presented here using material parameters generated from the Varga strain energy function. The Varga strain energy function takes the form

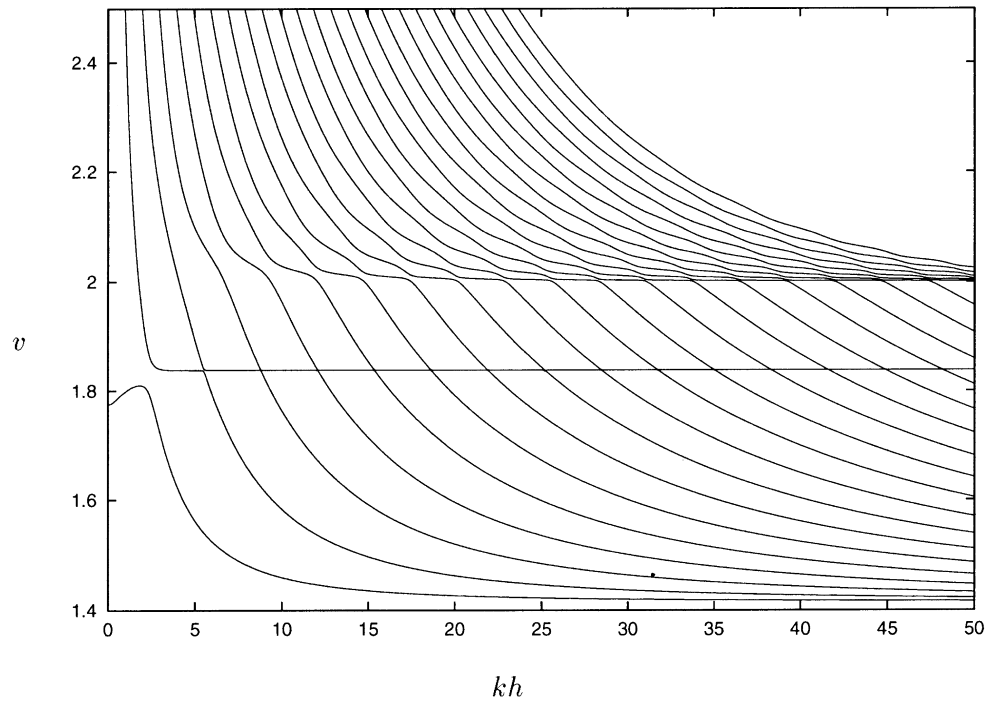

Fig. 2. Phase speed against scaled wave numbers for Mooney–Rivlin materials 2 and 1 from Table 1 in the outer layers and inner core, respectively, and $\sigma_2 = 1.8$, with $v_R = 1.8378$, no real v_I, $v_{S_1} = 2.0, 1.414$, $v_{S_2} = 1.732$ and no real $\tilde{v}_{S_2}$.

$$W = \mathscr{C}_1(\lambda_1 + \lambda_2 + \lambda_3 - 3), \tag{3.2}$$

where $\mathscr{C}_1$ is a shear modulus. The two Varga materials used in next figures in both the inner core and outer layers are denoted by material 3 and 4, and are summarised with the appropriate material constants are in Table 1.

Fig. 3 shows the first twenty five branches of the dispersion relation (2.12) for a laminate formed of material 3 in the outer layers and material 4 in the inner core. For these material parameters the high wave number phase speed limit of the fundamental mode and all harmonics is $\tilde{v}_{S_2}$, a second shear wave in the inner core. This behaviour we will refer to as Case 3. In this case within the high wave number it is known that p_1 and p_2 are both imaginary, with $|p_1| \to |p_2|$ as $kh, kd \to \infty$, whilst q_1 and q_2 are either both real or complex conjugates. Accordingly the high wave number limit is obtained by setting the discriminant of the appropriate form of (2.6) to zero, to obtain

$$\tilde{\rho}\,\tilde{v}_{S_2}^2 = 2\tilde{\beta} - 2\tilde{\gamma} + 2\sqrt{\tilde{\gamma}}\sqrt{\tilde{\alpha} + \tilde{\gamma} - 2\tilde{\beta}}, \tag{3.3}$$

where a similar shear wave speed v_{S_2} associated with the outer layers is also noted. In Fig. 3 the harmonics flatten together to form ghost lines at various values of the phase speed. Two of these values are associated with the first shear wave speed values in the inner core ($\tilde{v}_{S_1} = 1.876$) and the outer layers ($v_{S_1} = 2.012$). The third ghost line is formed around the value of $v \approx 1.936$ and appears to be associated with the material parameters of the inner core (material 4). This ghost line is not associated with the values of the three shear wave speeds $v_{S_1}, \tilde{v}_{S_1}, \tilde{v}_{S_2}$ or v_{S_2} nor with the surface save speed v_R. It has been

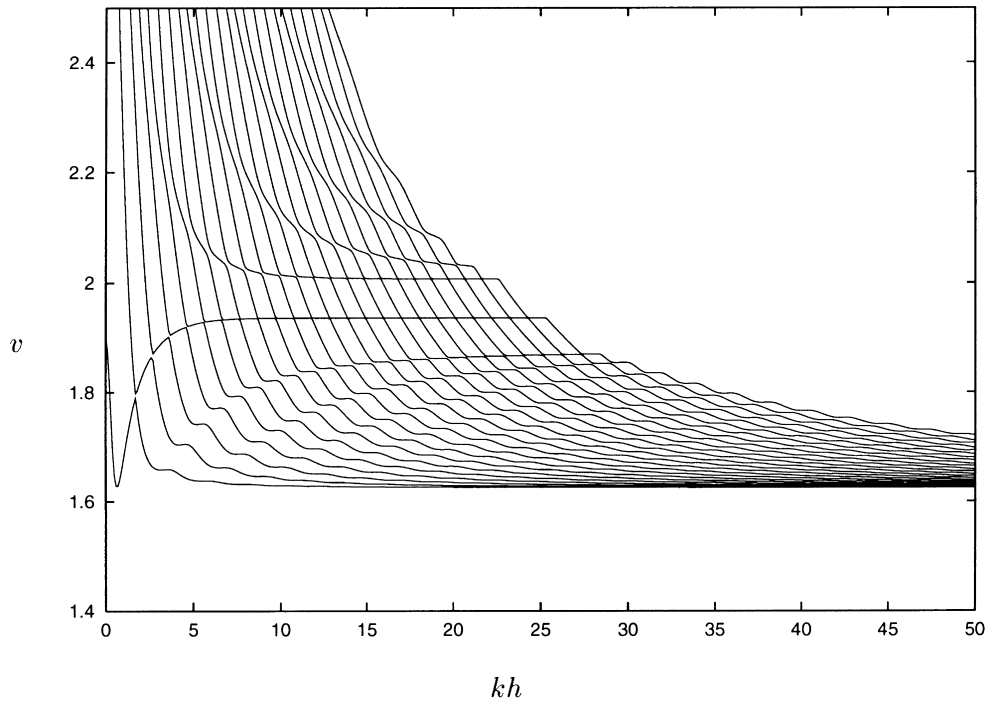

Fig. 3. Phase speed against scaled wave number for Varga materials 3 and 4 from Table 1 in the outer layers and inner core, respectively, and $\sigma_2 = 1.0$, with $v_R = 2.0068$, no real v_1, $v_{S_1} = 2.012, \tilde{v}_{S_1} = 1.876$, $v_{S_2} = 1.897$ and $\tilde{v}_{S_2} = 1.625$.

verified numerically that there is no such flattening of the dispersion curves around this value for a single layer plate formed of the same material, and this is therefore a feature of multi-layered media. The reason for formation of such flattening around this wave speed value therefore appears complex and, as such, is left for future work. For wave speeds below the ghost line associated with $\tilde{v}_{S_1}$ (= 1.876) there exists oscillatory behaviour in the fundamental mode and harmonics.

A final graph of dispersion curves for extensional waves is shown in Fig. 4. For this graph materials 3 and 4 from Table 1 have been used for the inner core and outer layers, respectively. These parameters yield a surface wave with speed $v_R = 1.3067$ as the high wave number limit of the fundamental mode, with the corresponding limit of the harmonics being $v_{S_2} = 1.625$. This behaviour corresponds to Case 4 and thus numerically we have that q_1 and q_2 are both imaginary, with $|q_1| \to |q_2|$ as $kh \to \infty$, whilst p_1 and p_2 are either both real or complex conjugates. There is flattening of the dispersion curves associated with the remaining shear wave speeds, $v_{S_1} = 1.876$, $\tilde{v}_{S_1} = 2.012$ and $v \approx 1.936$, with the sharpest flattening occurring around this last value. The harmonics exhibit oscillatory behaviour for phase speeds less than v_{S_1}, with the harmonics apparently grouping together in pairs.

4. An asymptotic analysis

We shall now investigate the numerical indications discussed in the previous section analytically in respect of arbitrary strain energy functions. Specifically an asymptotic analysis in both the high and low wave number regions is carried out.

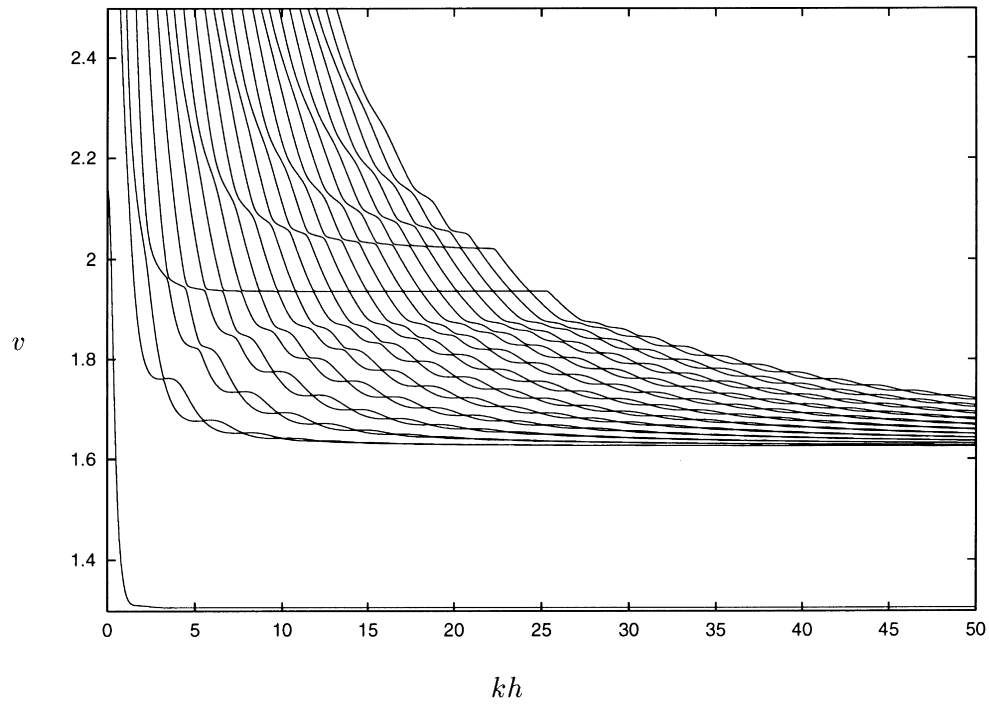

Fig. 4. Phase speed against scaled wave number for Varga materials 4 and 3 from Table 1 in the outer layers and inner core, respectively, and $\sigma_2 = 0.5$, with $v_R = 1.3067$, no real v_I, $v_{S_1} = 1.876$, $v_{S_2} = 1.625$, $\tilde{v}_{S_1} = 2.012$ and $\tilde{v}_{S_2} = 1.732$.

4.1. Long wavelength limit (kh → 0)

The long wave limit is investigated by allowing $kh, kd \to 0$ in the dispersion relation. The numerical results obtained indicate that only the fundamental mode retains a finite wave speed in the limit, and therefore the limit $kh, kd \to 0$ of the dispersion relation (2.12) is first taken whilst assuming that the speed of wave propagation remains finite. The leading order term of eqn (2.12) in the long wave limit is given by

$$2q_1q_2f(q_1)f(q_2)\delta_1^{(0)} + q_1f(q_2)^2\{-kq_2h\delta_2^{(0)} + \delta_3^{(0)}\} - q_2f(q_1)^2\{kq_1h\delta_2^{(0)} - \delta_4^{(0)}\} + O(k^2) = 0, \tag{4.1}$$

within which

$$\begin{aligned}
\delta_1^{(0)} &= p_1\{\tilde{f}(p_2) - f(q_2)\}\{f(q_1) - \tilde{f}(p_2)\}kp_2d + p_2\{\tilde{f}(p_1) - f(q_2)\}\{\tilde{f}(p_1) - f(q_1)\}kp_1d,\\
\delta_2^{(0)} &= p_1p_2\{f(q_2) - f(q_1)\}\{\tilde{f}(p_1) - \tilde{f}(p_2)\},\\
\delta_3^{(0)} &= p_1q_2\{\tilde{f}(p_2) - f(q_1)\}^2kp_2d - p_2q_2\{\tilde{f}(p_1) - f(q_1)\}^2kp_1d,\\
\delta_4^{(0)} &= p_2q_1\{\tilde{f}(p_1) - f(q_2)\}^2kp_1d - p_1q_1\{\tilde{f}(p_2) - f(q_2)\}^2kp_2d.
\end{aligned} \tag{4.2}$$

After some algebraic manipulation eqn (4.1) may be simplified to

$$d\{f(q_1) - f(q_2)\}^2\{\tilde{f}(p_1)^2 - \tilde{f}(p_2)^2\} + h\{\tilde{f}(p_1) - \tilde{f}(p_2)\}^2\{f(q_1)^2 - f(q_2)^2\} = 0. \tag{4.3}$$

It is clear that eqn (4.3) possesses two common factors in each of the terms, namely $\{\tilde{f}(p_1)-\tilde{f}(p_2)\}$ and $\{f(q_1)-f(q_2)\}$. Both of these factors correspond to spurious roots of the dispersion relation associated with the double roots $p_1^2=p_2^2$ and $q_1^2=q_2^2$, respectively. These roots are spurious in the sense that they lead to non-dispersive shear wave speeds. On removing the spurious roots and making use of the appropriate forms of eqn (2.7), the long wave speed of the fundamental mode may be obtained in the form

$$v=\sqrt{\frac{2\left(\tilde{\beta}+\tilde{\gamma}-\sigma_2\right)+2(\beta+\gamma-\sigma_2)}{\tilde{\rho}\,d+\rho h}}. \tag{4.4}$$

4.2. Surface and interfacial waves

Our numerical calculations indicated that the high wave number limiting behaviour of the dispersion relation depends on whether p_1, p_2, q_1 and q_2 are real, imaginary or complex conjugates. If we first consider the case when p_1 and p_2, and q_1 and q_2 are either purely real or complex conjugates, then in the limit $kh, kd\to\infty$ the dispersion relation (2.12) tends to

$$\left\{q_1 f(q_2)^2-q_2 f(q_1)^2\right\}\left\{\delta_2^{(\infty)}-\delta_3^{(\infty)}-\delta_4^{(\infty)}+\delta_5^{(\infty)}\right\}=0, \tag{4.5}$$

in which a superscript (∞) indicates that we have divided the dispersion relation by appropriate hyperbolic functions and the resultant hyperbolic tangents have been replaced with unity. It may readily be shown that these two factors yield the Rayleigh surface wave equation ($R(v)=0$) and the Stoneley interfacial wave equation ($S(v)=0$), see Dowaikh and Ogden (1990) and Dowaikh and Ogden (1991), respectively. Whether such waves exist in a particular case is dependent on the material parameters and on the Cauchy stress σ_2 in the case of surface waves. If real solutions of both equations exist in general the fundamental mode and first harmonic will tend to one of each in order of increasing magnitude, however in the numerical section a situation was observed in which a valid surface wave speed exists but is not a high wave number limiting wave speed. This will be further discussed in a later section.

4.3. Short wavelength limit of the harmonics ($\mathrm{kh}\to\infty$)

In general, with the possible exception of the first, all harmonics will tend to the lower of two shear wave speeds associated with the inner core and the outer layers. The value of the limiting wave speed in the outer layers will take one of two values depending on the material parameters, specifically the relative magnitudes of α and 2β. The first limiting wave speed arises when $\alpha\leqslant 2\beta$ and numerically it is known that one of q_1 and q_2 is imaginary, the other remaining real. If $q_1=i\hat{q}_1$ then $|\hat{q}_1|\to 0$ as $kh, kd\to\infty$. The second case arises when $\alpha>2\beta$ and it is seen numerically that both q_1 and q_2 are imaginary and that $|q_1|\to|q_2|$ as $kh, kd\to\infty$. The limiting wave speed in the outer layer may therefore be written explicitly as

$$\rho v_L^2=\begin{cases}\rho v_{S_1}^2=\alpha & \alpha\leqslant 2\beta\\ \rho v_{S_2}^2=2\beta-2\gamma+2\sqrt{\gamma}\sqrt{\alpha+\gamma-2\beta} & \alpha>2\beta\end{cases}, \tag{4.6}$$

with the corresponding limiting wave speed for the inner core given by

$$\tilde{\rho}\,\tilde{v}_L^2 = \begin{cases} \tilde{\rho}\,\tilde{v}_{S_1} = \tilde{\alpha} & \tilde{\alpha} \leqslant 2\tilde{\beta} \\ \tilde{\rho}\,\tilde{v}_{S_2} = 2\tilde{\beta} - 2\tilde{\gamma} + 2\sqrt{\tilde{\gamma}}\sqrt{\tilde{\alpha} + \tilde{\gamma} - 2\tilde{\beta}} & \tilde{\alpha} > 2\tilde{\beta} \end{cases}. \tag{4.7}$$

In general the limiting wave speed for the outer layers (inner core) will be the minimum of v_{S_1} and v_{S_2} ($\tilde{v}_{S_1}$ and $\tilde{v}_{S_2}$). However, in certain situations it is possible for v_{S_1} ($\tilde{v}_{S_1}$) to be the limiting wave speed when $v_{S_2} < v_{S_1}$ ($\tilde{v}_{S_2} < \tilde{v}_{S_1}$). This point may be elucidated by considering the situation in which q_1 and q_2 are complex conjugates, namely that $q_1 = q_r + iq_i$ and $q_2 = q_r - iq_i$, where $q_r, q_i > 0$. Under this specialisation eqn (2.7) becomes

$$2\gamma\left(q_r^2 - q_i^2\right) = 2\beta - \rho v^2, \quad \gamma\left(q_r^2 + q_i^2\right)^2 = \alpha - \rho v^2. \tag{4.8}$$

As q_r and q_i are real and positive in eqn (4.8) it is inferred that the region in which q_1 and q_2 are complex is restricted by $\alpha > \rho v^2$ and explicit representations of q_r and q_i are deduced to be

$$q_r^2 = \frac{2\beta - \rho v^2}{4\gamma} + \sqrt{\frac{\alpha - \rho v^2}{4\gamma}}, \quad q_i^2 = \frac{\rho v^2 - 2\beta}{4\gamma} + \sqrt{\frac{\alpha - \rho v^2}{4\gamma}}. \tag{4.9}$$

The limit $v \to v_{S_2}$ as $kh \to \infty$ occurs as the discriminant of eqn (2.6) vanishes. This may arise in one of two ways, the first occurs when $q_1 \to -q_2$, corresponding to q_r vanishing and q_1 and q_2 both being imaginary, whilst the second occurs when $q_1 \to q_2$, corresponding to q_r vanishing and q_1 and q_2 both being real. It should be noted that v_{S_2} will only be a valid limiting wave speed in the case when q_1 and q_2 are both imaginary. When q_1 and q_2 are real the only valid limiting wave speeds of the dispersion equation are those given be the Rayleigh surface wave equation and the Stoneley interfacial equation. If $q_r = 0$ then from eqn (4.9) we have

$$\frac{\rho v_{S_2}^2 - 2\beta}{4\gamma} = \sqrt{\frac{\alpha - \rho v_{S_2}^2}{4\gamma}} > 0, \tag{4.10}$$

from which it is inferred that $\rho v_{S_2}^2 > 2\beta$, and on making use of the definitions of v_{S_2} this condition becomes $\alpha < 2\beta$ and the region within which v_{S_2} can lie given by $2\beta < \rho v_{S_2}^2 < \alpha$. If $q_i = 0$ then from eqn (4.9) we have

$$\frac{2\beta - \rho v_{S_2}^2}{4\gamma} = \sqrt{\frac{\alpha - \rho v_{S_2}^2}{4\gamma}} > 0, \tag{4.11}$$

from which it is deduced that $\alpha > 2\beta$. It is clear from eqn (4.6) that a real value of v_{S_2} will only exist if $\alpha + \gamma > 2\beta$. This condition is automatically satisfied in the case when $\alpha > 2\beta$. It is then clear that in general there are four possible wave speed limits for the harmonics as $kh, kd \to \infty$, the actual limit therefore being dependent on the material parameters. Each possible limit is now analysed in turn.

Case 1: $v \to v_{S_1}$ with $2\beta \geqslant \alpha$ and $v_{S_1}^2 < \tilde{\rho}\,\tilde{v}_L^2$

In the Case 2 $\beta \geqslant \alpha$ and $\rho v_{S_1}^2 < \tilde{\rho}\,\tilde{v}_L^2$ numerical calculations indicate that for all harmonics ρv^2 will in general approach α from above and therefore, from eqn (2.6), only one of q_1 and q_2 is real, the other being purely imaginary, with p_1 and p_2 either real or complex conjugates. It is assumed, without loss of generality, that $q_1 = i\hat{q}_1$, where $\hat{q}_1 \geqslant 0$ is real, and $\hat{q}_1 \to 0$ as $kh, kd \to \infty$. It is reiterated that the inequality $2\beta \geqslant \alpha$ precludes v_{S_2} from being a valid limit for the harmonics even if v_{S_2} exists and $v_{S_2} < v_{S_1}$. Accordingly we seek to expand the dispersion relation (2.12) around the small order quantity $\hat{q}_1$. Using eqn (2.6) an expansion for the phase speed is obtained, thus

$$\rho v^2 = \left(\gamma\hat{q}_1^4 + 2\beta\hat{q}_1^2 + \alpha\right)\left(1+\hat{q}_1^2\right)^{-1}$$
$$= \alpha + \hat{q}_1^2(2\beta-\alpha) + \hat{q}_1^4(\alpha+\gamma-2\beta) + O\left(\hat{q}_1^6\right). \tag{4.12}$$

Similar expansions for q_2, p_1 and p_2 are then obtained using eqn (4.12) with the appropriate form of eqn (2.6), namely

$$q_2 = q_2^{(0)} + O\left(\hat{q}_1^2\right), \quad p_1 = p_1^{(0)} + O\left(\hat{q}_1^2\right), \quad p_2 = p_2^{(0)} + O\left(\hat{q}_1^2\right), \tag{4.13}$$

within which $q_2^{(0)}$, $p_1^{(0)}$ and $p_2^{(0)}$ are order 1 quantities defined by

$$q_2^{(0)} = \sqrt{\frac{2\beta-\alpha}{\gamma}},$$

$$p_1^{(0)^2}, \quad p_2^{(0)^2} = \frac{1}{2\tilde{\gamma}}\left\{2\tilde{\beta} - \frac{\tilde{\rho}\alpha}{\rho} \pm \sqrt{\left(2\tilde{\beta} - \frac{\tilde{\rho}\alpha}{\rho}\right)^2 - 4\tilde{\gamma}\left(\tilde{\alpha} - \frac{\tilde{\rho}\alpha}{\rho}\right)}\right\}. \tag{4.14}$$

On making use of eqns (4.12)–(4.14) the associated form of the dispersion relation for extensional waves (2.12), appropriate for large *kh, kd*, then takes the form

$$\tan\left(k\hat{q}_1 h\right)\left\{\left[(\gamma-\sigma_2)^2 q_2^{(0)}\eta_1 + O\left(\hat{q}_1^2\right)\right] - \hat{q}_1^2\left[\left(\gamma\left(q_2^{(0)^2}+1\right)-\sigma_2\right)^2\zeta_1 + O\left(\hat{q}_1^2\right)\right]\right\}$$
$$= \hat{q}_1\left\{\left(\gamma\left(q_2^{(0)^2}+1\right)-\sigma_2\right)^2\eta_1 + (\gamma-\sigma_2)^2 q_2^{(0)}\zeta_1 + O\left(\hat{q}_1^2\right)\right\}, \tag{4.15}$$

within which η_1 and ζ_1 are order 1 quantities defined as

$$\eta_1 = p_1^{(0)}q_2^{(0)}\left\{\gamma - \tilde{\gamma}\left(p_2^{(0)^2}+1\right)\right\}^2 - p_2^{(0)}q_2^{(0)}\left\{\gamma - \tilde{\gamma}\left(p_1^{(0)^2}+1\right)\right\}^2 + p_1^{(0)}p_2^{(0)}q_2^{(0)}\left(p_2^{(0)^2} - p_1^{(0)^2}\right)\gamma\tilde{\gamma}, \tag{4.16}$$

$$\zeta_1 = p_1^{(0)}\left\{\gamma\left(q_2^{(0)^2}+1\right) - \tilde{\gamma}\left(p_2^{(0)^2}+1\right)\right\}^2 - q_2^{(0)^3}\left(p_2^{(0)^2} - p_1^{(0)^2}\right)\gamma\tilde{\gamma} - p_2^{(0)}\left\{\gamma\left(q_2^{(0)^2}+1\right) - \tilde{\gamma}\left(p_1^{(0)^2}+1\right)\right\}^2. \tag{4.17}$$

It is clear from eqn (4.15) that the leading-order term will change if $\gamma = \sigma_2$ and we will therefore consider the two cases $\gamma \neq \sigma_2$ and $\gamma = \sigma_2$ separately.

(i) $\gamma \neq \sigma_2$

In the case when $\gamma \neq \sigma_2$ the leading-order terms of eqn (4.15) now yield

$$\tan\left(k\hat{q}_1 h\right)\left\{(\gamma-\sigma_2)^2 q_2^{(0)}\eta_1 + O\left(\hat{q}_1^2\right)\right\} = \hat{q}_1\left\{\left(\gamma\left(q_2^{(0)^2}+1\right)-\sigma_2\right)^2\eta_1 + (\gamma-\sigma_2)^2 q_2^{(0)}\zeta_1 + O\left(\hat{q}_1^2\right)\right\}. \tag{4.18}$$

From eqn (4.18) it is deduced that $O(1)\tan\left(k\hat{q}_1 h\right) \sim O(\hat{q}_1)$, implying that $\tan\left(k\hat{q}_1 h\right) \to 0$ as $\hat{q}_1 \to 0$, and therefore,

$$\hat{q}_1 = \frac{n\pi}{kh} + O(kh)^{-2}. \tag{4.19}$$

Inserting eqn (4.19) into eqn (4.12) yields the second-order approximation to the phase speed of the nth harmonic

$$\rho v_n^2 = \alpha + (2\beta - \alpha)\left(\frac{n\pi}{kh}\right)^2 + \cdots, \quad n = 1, 2, 3, \ldots . \tag{4.20}$$

A higher-order expansion for the phase speed is obtained by setting

$$\hat{q}_1 = \frac{n\pi}{kh} + \frac{\phi_1}{(kh)^2} + O(kh)^{-3}, \quad \tan\left(k\hat{q}_1 h\right) = \frac{\phi_1}{kh} + O(kh)^{-3}, \tag{4.21}$$

in which ϕ_1 is to be determined. If these two expansions are inserted into eqn (4.18) and like powers of kh equated it is found that

$$\phi_1 = \left\{ \frac{\left\{\gamma\left(q_2^{(0)^2} + 1\right) - \sigma_2\right\}^2}{q_2^{(0)}(\gamma - \sigma_2)^2} + \frac{\zeta_1}{\eta_1} \right\} n\pi. \tag{4.22}$$

On inserting eqn (4.22) into eqn $(4.21)_1$, and on making use of eqn (4.12), it may be shown that

$$\rho v_n^2 = \alpha + (2\beta - \alpha)\left(\frac{n\pi}{kh}\right)^2 \left\{ 1 + \frac{2}{kh} \left\{ \frac{\left\{\gamma\left(q_2^{(0)^2} + 1\right) - \sigma_2\right\}^2}{q_2^{(0)}(\gamma - \sigma_2)} + \frac{\zeta_1}{\eta_1} \right\} \right\} + \cdots, \quad n = 1, 2, 3, \ldots . \tag{4.23}$$

A comparison of the asymptotic expansions obtained in eqn (4.23) with numerical solutions of the dispersion relation (2.12) is presented in Fig. 5 for the same material parameters used in Fig. 1. Fig. 5 indicates good agreement between the asymptotic expansions and the numerical solutions in the high wave number regime. As may be expected, the value of scaled wave number at which this good agreement is obtained increases as the harmonic number increases, i.e., as n increases. It is noted that expansions for large n and moderate wave number have been obtained for a single plate by Rogerson (1997). Whilst in theory such expansions could be obtained for the symmetric 4-ply plate, the increased algebraic complexity makes the derivation of these difficult and time consuming to obtain without resort to a computer manipulation package.

(ii) $\gamma = \sigma_2$

In the case in which $\gamma = \sigma_2$ the leading-order term of the dispersion relation changes and may be deduced from eqn (4.15) to be

$$-\hat{q}_1^2 \tan\left(k\hat{q}_1 h\right)\left\{\zeta_1 + O\left(\hat{q}_1^2\right)\right\} = \hat{q}_1\left\{\eta_1 + O\left(\hat{q}_1^2\right)\right\}, \tag{4.24}$$

from which it is readily inferred that $O(\hat{q}_1)\tan\left(k\hat{q}_1 h\right) \sim O(1)$ implying that $\tan\left(k\tilde{q}_1 h\right) \to \infty$ as $kh \to \infty$. Accordingly expansions for the phase speed are sought by setting

$$\hat{q}_1 = \left(n + \frac{1}{2}\right)\pi + \frac{\phi_1^*}{(kh)^2} + O(kh)^{-3}, \quad \tan\left(k\hat{q}_1 h\right) = -\frac{kh}{\phi_1^*} + O(kh)^{-1}, \tag{4.25}$$

where ϕ_1^* is to be determined. On inserting the expansions shown in eqn (4.25) into eqn (4.24), and by examine leading-order terms, it is found that

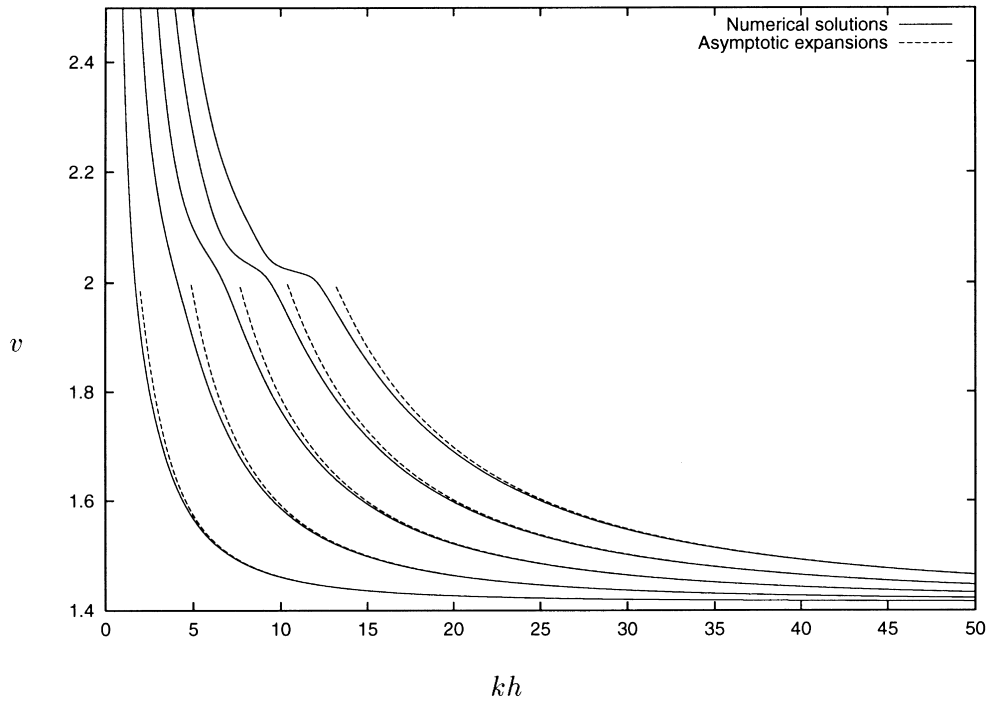

Fig. 5. Comparison of numerical solutions with asymptotic expansions obtained for Case 1, see eqn (4.23). The same material parameters from Fig. 1 are used.

$$\phi_1^* = \frac{\zeta_1}{\eta_1}\left(n+\frac{1}{2}\right)\pi. \tag{4.26}$$

Finally, inserting eqn (4.26) into eqn $(4.25)_1$ and by making use of eqn (4.12), the third-order expansion of the phase speed in this case is found, namely

$$\rho v_n^2 = \alpha + (2\beta-\alpha)\left(n+\frac{1}{2}\right)^2\left(\frac{\pi}{kh}\right)^2\left\{1+\frac{2}{kh}\frac{\zeta_1}{\eta_1}\right\}+\cdots,\ n=1,2,3\ldots\ . \tag{4.27}$$

It is interesting to note in eqn (4.23) and (4.27) that n is replaced by $(n+1/2)$ in the second- (and higher)-order terms.

The asymptotic representations shown in eqn (4.23) have been obtained previously for the analogous flexural wave problem in this particular case, see Rogerson and Sandiford (1997, eqn (4.40)). The same expansion is obtained for both the flexural and extensional dispersion relations as the two dispersion relations differ only by subtle permutation of the hyperbolic functions associated with the inner core, namely $\tilde{C}_m \to \tilde{S}_m$ and $\tilde{S}_m \to \tilde{C}_m (m=1,2)$. The two dispersion relations therefore have the same limiting behaviour when p_1 and p_2 are both real or form a complex conjugate pair (i.e. when the limiting behaviour of $\tanh kp_m d$ is well defined for large wave number). This is examined further in a later section when numerical solutions of the extensional and flexural dispersion relations are compared.

Case 2: $v \to \tilde{v}_{S_1}$ when $2\tilde{\beta} \geqslant \tilde{\alpha}$ and $\tilde{\rho}\,\tilde{v}_{S_1}^2 < \rho v_L^2$

By a similar argument to the previous case $\tilde{\rho}\,v^2 \to \tilde{\alpha}$ from above and hence only one of p_1 and p_2 is imaginary, with q_1 and q_2 both real or a complex conjugate pair. If $p_1 = i\hat{p}_1$, where $\hat{p}_1 \geqslant 0$ then as $kh, kd \to \infty$, $\hat{p}_1 \to 0$ and accordingly we expand the dispersion relation (2.12) around this small quantity

$\hat{p}_1$. The analogous forms of eqn (4.13) are now given by

$$p_2 = p_2^{(0)} + O\left(\hat{p}_1^2\right), \quad q_1 = q_1^{(0)} + O\left(\hat{p}_1^2\right), \quad q_2 = q_2^{(0)} + O\left(\hat{p}_1^2\right),$$

where $p_2^{(0)}$, $q_1^{(0)}$ and $q_2^{(0)}$ maybe inferred from eqn (4.14). On making use of these expansions and allowing kh, kd to be large, the dispersion relation factorises into two components, thus either

$$q_1^{(0)} f\left(q_2^{(0)}\right)^2 - q_2^{(0)} f\left(q_1^{(0)}\right)^2 + O\left(\hat{p}_1^2\right) = 0, \tag{4.28}$$

or

$$\tan k\hat{p}_1 d\left\{\zeta_2 + O\left(\hat{p}_1^2\right)\right\} = \hat{p}_1\left\{\eta_2 + O\left(\hat{p}_1^2\right)\right\}, \tag{4.29}$$

where η_2 and ζ_2 are order 1 quantities defined as

$$\zeta_2 = p_2^{(0)} q_2^{(0)}\left\{\tilde{\gamma} - \gamma\left(q_1^{(0)^2} + 1\right)\right\}^2 - p_2^{(0)} q_1^{(0)}\left\{\tilde{\gamma} - \gamma\left(q_2^{(0)^2} + 1\right)\right\}^2 - p_2^{(0)} q_1^{(0)} q_2^{(0)}\left\{q_2^{(0)^2} - q_1^{(0)^2}\right\}, \tag{4.30}$$

$$\eta_2 = q_2^{(0)}\left\{\tilde{\gamma}\left(p_2^{(0)^2} + 1\right) - \gamma\left(q_2^{(0)^2} + 1\right)\right\}^2 - q_1^{(0)}\left\{\tilde{\gamma}\left(p_2^{(0)^2} + 1\right) - \gamma\left(q_2^{(0)} + 1\right)\right\}^2 + p_2^{(0)^3}\left\{q_2^{(0)^2} - q_1^{(0)^2}\right\}. \tag{4.31}$$

Eqn (4.28), to leading order, corresponds to $R(\tilde{v}_{S_1}) = 0$ and therefore is not a valid limit except in the exceptional case $v_R = \tilde{v}_{S_1}$. However, in such cases in which a Rayleigh surface wave speed exists and is greater than the limiting wave speed of the harmonics a surface wave front may be formed from the combined contribution of harmonics, see later in Figs 9 and 10.

From eqn (4.29) it is readily deduced that $O(1)\tan k\hat{p}_1 d \sim O(\hat{p}_1)$, implying that $\tan k\hat{p}_1 d \to 0$ as $\hat{p}_1 \to 0$ in the limit kh, $kd \to \infty$, therefore

$$\hat{p}_1 = \frac{n\pi}{kd} + O(kd)^{-2}. \tag{4.32}$$

The second-order approximation to the phase speed is obtained by inserting eqn (4.32) into the appropriate form of (4.12), yielding

$$\tilde{\rho}\, v_n^2 = \tilde{\alpha} + \left(2\tilde{\beta} - \tilde{\alpha}\right)\left(\frac{n\pi}{kd}\right)^2 + \cdots, \quad n = 1, 2, 3, \ldots . \tag{4.33}$$

A third-order approximation is then sought by setting

$$\hat{p}_1 = \frac{n\pi}{kd} + \frac{\phi_2}{(kd)^2} + O(kd)^{-3}, \quad \tan k\hat{p}_1 d = \frac{\phi_2}{kd} + O(kd)^{-3}, \tag{4.34}$$

where ϕ_2 is to be determined. On inserting eqn (4.34) into (4.29) and comparing like powers of kd it is readily deduced that

$$\phi_2 = \frac{\eta_2}{\zeta_2} n\pi. \tag{4.35}$$

Finally inserting eqns (4.35) and $(4.34)_1$ into equation the appropriate form of (4.12) gives rise to the third-order expansion of the phase speed, namely

$$\tilde{\rho}\, v_n^2 = \tilde{\alpha} + (2\tilde{\beta} - \tilde{\alpha})\left(\frac{n\pi}{kd}\right)^2 \left\{1 + \left(\frac{2}{kd}\right)\frac{\eta_2}{\zeta_2}\right\} + \cdots, \quad n = 1, 2, 3, \ldots . \tag{4.36}$$

A comparison of the numerical solutions and the asymptotic expansions is given in Fig. 6 which shows the asymptotic expansions generated from eqn (4.36) superimposed upon the first seven harmonics of the dispersion curves shown in Fig. 2. The figure indicates exceptional agreement between the asymptotic and numerical solutions. It is interesting to note that the asymptotic expansions associated with the nth harmonics provides a reasonable approximation until the flattening of the dispersion curves around v_R. Above this flattening the expansions for the nth harmonics appears to follow the $(n + 1)$th harmonic.

Case 3: $v \to \tilde{v}_{S_2}$ when $2\tilde{\beta} < \tilde{\alpha}$ and $\tilde{\rho}\,\tilde{v}_{S_2}^2 < \rho v_L^2$

The limit $v \to \tilde{v}_{S_2}$ arises when the material parameters are such that $2\tilde{\beta} < \tilde{\alpha}$ and $\tilde{\rho}\,\tilde{v}_{S_2}^2 < \rho v_L^2$. Numerical calculations guide us in assuming that as $kh, kd \to \infty$ both p_1 and p_2 are imaginary, with $|p_1| \to |p_2|$, whilst q_1 and q_2 are either real or complex conjugates. The limit $kh, kd \to \infty$ may therefore be examined in this case be setting

$$p_1^2 = -\tilde{a} + \tilde{b}, \quad p_2^2 = -\tilde{a} - \tilde{b}, \quad \tilde{a} > 0, \quad \tilde{b} \geqslant 0, \tag{4.37}$$

where $\tilde{a}$ and $\tilde{b}$ are real and $\tilde{b} \to 0$ as $kh, kd \to \infty$. The implication is that $\tilde{\rho}\, v^2 \to \tilde{\rho}\,\tilde{v}_{S_2}^2$ from above and it may be easily deduced from the appropriate form of eqn (2.7) that the region in which (4.37) is valid is $\tilde{\rho}\,\tilde{v}_{S_2}^2 < \tilde{\rho}\, v^2 < \tilde{\alpha}$. The values of $\tilde{a}$ and $\tilde{b}$ may be obtained explicitly from the appropriate form of eqn (2.6), thus,

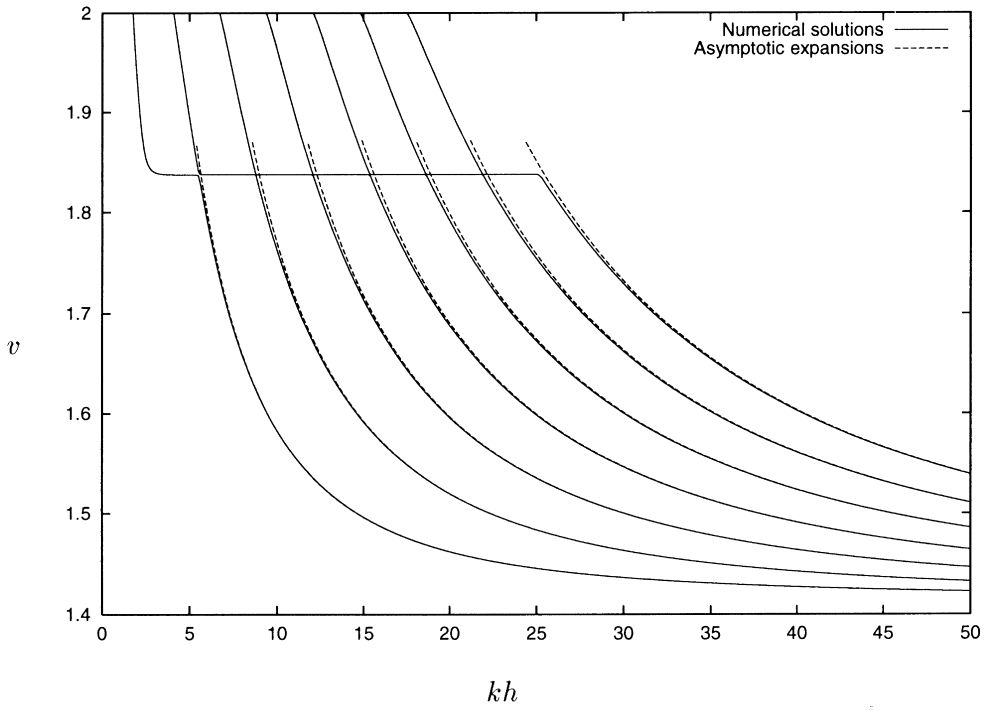

Fig. 6. Comparison of numerical solutions with asymptotic expansions obtained for Case 2, see eqn (4.36). The same material parameters from Fig. 2 are used.

$$\tilde{a} = \frac{\tilde{\rho}\, v^2 - 2\tilde{\beta}}{2\tilde{\gamma}}, \quad \tilde{b} = \frac{\sqrt{\left(2\tilde{\beta} - \tilde{\rho}\, v^2\right)^2 - 4\tilde{\gamma}\left(\tilde{\alpha} - \tilde{\rho}\, v^2\right)}}{2\tilde{\gamma}}. \tag{4.38}$$

If the forms of p_1^2 and p_2^2 shown in eqn (4.37) are inserted into the appropriate form of eqn (2.7) it is observed that $\tilde{a}$ may be expanded in terms of $\tilde{b}$ to obtain

$$\tilde{a} = \tilde{a}_0 + \tilde{a}_1 \tilde{b}^2 + O\left(\tilde{b}^4\right), \tag{4.39}$$

where

$$\tilde{a}_0 = -1 + \tilde{\gamma}^{1/2}\left(\tilde{\alpha} + \tilde{\gamma} - 2\tilde{\beta}\right)^{1/2}, \quad \tilde{a}_1 = \frac{1}{2(\tilde{a}_0 + 1)}, \tag{4.40}$$

and it is noted that the existence of a real $\tilde{a}_0$ in eqn $(4.40)_1$ is guaranteed in view of the fact $\tilde{\alpha} > 2\tilde{\beta}$. The high wave number limit of the dispersion relation is investigated by allowing $kh, kd \to \infty$ in eqn (2.12) and expanding all terms around the small-order quantity $\tilde{b}$. It is observed that in this limit the dispersion relation comprises of two factors, namely

$$q_1^{(0)} f\left(q_2^{(0)}\right)^2 - q_2^{(0)} f\left(q_1^{(0)}\right)^2 + O\left(\tilde{b}^2\right) = 0, \tag{4.41}$$

or

$$\begin{aligned} \gamma\tilde{\gamma}\left(q_2^{(0)^2} - q_1^{(0)^2}\right)\left(q_1^{(0)} q_2^{(0)} - \tilde{a}_0\right)\tilde{b}\, C(\tilde{a}_0) - \left\{\sqrt{\tilde{a}_0}\chi^{(1)} - \frac{\chi^{(0)}}{\sqrt{2\tilde{a}_0}}\right\}\tilde{b}\, S(\tilde{a}_0) \\ = \sqrt{\tilde{a}_0}\chi^{(0)} S(\tilde{b}) - \gamma\tilde{\gamma}\left(q_2^{(0)^2} - q_1^{(0)^2}\right)\left(q_1^{(0)} q_2^{(0)} + \tilde{a}_0\right)\tilde{b}\, C(\tilde{b}) + O\left(\tilde{b}^2\right), \end{aligned} \tag{4.42}$$

within which

$$\begin{aligned} \chi^{(0)} &= q_2^{(0)}\left\{\gamma\left(q_1^{(0)^2} + 1\right) + \tilde{\gamma}(\tilde{a}_0 - 1)\right\}^2 - q_1^{(0)}\left\{\gamma\left(q_2^{(0)^2} + 1\right) + \tilde{\gamma}(\tilde{a}_0 - 1)\right\}^2, \\ \chi^{(1)} &= 2\tilde{\gamma}\left(q_2^{(0)}\left\{\gamma\left(q_1^{(0)^2} + 1\right) + \tilde{\gamma}(\tilde{a}_0 - 1)\right\} - q_1^{(0)}\left\{\gamma\left(q_2^{(0)^2} + 1\right) + \tilde{\gamma}(\tilde{a}_0 - 1)\right\}\right), \\ \chi^{(2)} &= \tilde{a}_1\chi^{(1)} + \tilde{\gamma}^2\left(q_2^{(0)} - q_1^{(0)}\right), \end{aligned}$$

$C(\tilde{a}_0)$, $S(\tilde{a}_0)$, $C(\tilde{b})$ and $S(\tilde{b})$ are trigonometric terms defined as

$$C(\tilde{a}_0) = \cos 2\sqrt{\tilde{a}_0}kd, \quad S(\tilde{a}_0) = \sin 2\sqrt{\tilde{a}_0}kd, \quad C(\tilde{b}) = \cos\left(\frac{\tilde{b}kd}{\sqrt{\tilde{a}_0}}\right), \quad S(\tilde{b}) = \sin\left(\frac{\tilde{b}kd}{\sqrt{\tilde{a}_0}}\right),$$

and $q_1^{(0)}$ and $q_2^{(0)}$ are order 1 terms which may be found by setting $v = \tilde{v}_{S_2}$ in eqn (2.6). To leading order, eqn (4.41) corresponds to $R(\tilde{v}_{S_2}) = 0$ and is therefore only a valid solution in the exceptional case in which $v_R = \tilde{v}_{S_2}$. It is observed from eqn (4.42) that $O(\tilde{b}) \sim O(1)S(\tilde{b})$, implying that $S(\tilde{b}) \to 0$ as $\tilde{b} \to 0$, and therefore

$$\tilde{b} = \sqrt{\tilde{a}_0}\frac{n\pi}{kd} + O(kd)^{-2}. \tag{4.43}$$

On inserting eqn (4.43) into eqn $(4.38)_1$, and making use of eqn (4.39), it is deduced that

$$\tilde{\rho}\, v_n^2 = 2\tilde{\beta} - 2\tilde{\gamma} + 2\tilde{\gamma}^{1/2}\left(\tilde{\alpha} + \tilde{\gamma} - 2\tilde{\beta}\right)^{1/2} + \left(\frac{n\pi}{kd}\right)^2 \left\{\frac{\tilde{\gamma}\tilde{a}_0}{\tilde{a}_0 + 1}\right\} + \cdots, \quad n = 1, 2, 3, \ldots . \tag{4.44}$$

A higher-order expansion for the phase speed is obtained by setting

$$\tilde{b} = \sqrt{\tilde{a}_0}\frac{n\pi}{kd} + \frac{\phi_3}{(kd)^2} + O(kd)^{-3}, \tag{4.45}$$

from which it is inferred that

$$\sin\left(\frac{\tilde{b}kd}{\sqrt{\tilde{a}_0}}\right) = (-1)^n \frac{\phi_3}{\sqrt{\tilde{a}_0}kd} + O(kd)^{-3}, \quad \cos\left(\frac{\tilde{b}kd}{\sqrt{\tilde{a}_0}}\right) = (-1)^n + O(kd)^{-2}, \tag{4.46}$$

where ϕ_3 is to be determined. On making use of eqns (4.45) and (4.46) in eqn (4.42), and comparing leading-order terms, it is deduced that

$$\phi_3 = (-1)^n \frac{\sqrt{\tilde{a}_0}}{2\chi^{(0)}} \left\{ \sqrt{\tilde{a}_0}\left(\frac{\chi^{(0)}}{\tilde{a}_0} - 2\chi^{(1)}\right) S(\tilde{a}_0) + 2\gamma\tilde{\gamma}\left(q_2^{(0)^2} - q_1^{(0)^2}\right)\left\{\left(q_1^{(0)}q_2^{(0)} - \tilde{a}_0\right)C(\tilde{a}_0) - (-1)^n\left(\tilde{a}_0 + q_1^{(0)}q_2^{(0)}\right)\right\}\right\} n\pi. \tag{4.47}$$

The expansion for the phase speed is then obtained to third order by making use of eqn (4.46), in conjunction with eqns (4.45), $(4.38)_1$ and (4.40), thus

$$\tilde{\rho}\, v_n^2 = 2\tilde{\beta} - 2\tilde{\gamma} + 2\tilde{\gamma}^{1/2}\left(\tilde{\alpha} + \tilde{\gamma} - 2\tilde{\beta}\right)^{1/2} + \left(\frac{n\pi}{kd}\right)^2 \left\{\frac{\tilde{\gamma}}{\tilde{a}_0 + 1}\right\}\left\{\tilde{a}_0 + \frac{2\sqrt{\tilde{a}_0}\hat{\phi}_3}{kd}\right\} + \cdots, \quad n = 1, 2, 3, \ldots, \tag{4.48}$$

and within which $\hat{\phi}_3 = \phi_3/n\pi$.

The asymptotic expansions obtained in eqn (4.48) are superimposed on numerical solutions in the next figure. The material parameters are taken from Fig. 3 as this affords a situation in which the limiting wave speed for the harmonics is $\tilde{v}_{S_2}$. Fig. 7 shows that the oscillatory behaviour of the harmonics in this limit are fully described by the trigonometric functions within the third-order term of the asymptotic expansions (4.44). These third-order expansions provide reasonable agreement with the numerical solutions even at a relatively low kh value.

Case 4: $v \to v_{S_2}$ when $2\beta < \alpha$ and $\rho v_{S_2}^2 < \tilde{\rho}\,\tilde{v}_L^2$

The final possible limiting wave speed arises when $\alpha > 2\beta$ and $\rho v_{S_2}^2 < \tilde{\rho}\,\tilde{v}_L^2$. Numerically it is known that there exists an analogous situation to that in the preceding section, in that both q_1 and q_2 are imaginary and $|q_1| \to |q_2|$ as $kh, kd \to \infty$, whilst p_1 and p_2 are either both real or complex conjugates. The limit $kh, kd \to \infty$ is therefore examined by setting

$$q_1^2 = -a + b, \quad q_2^2 = -a - b, \quad a > 0, b \geqslant 0, \tag{4.49}$$

where

$$a = \frac{\rho v^2 - 2\beta}{2\gamma}, \quad b = \frac{\sqrt{\left(2\beta - \rho v^2\right)^2 - 4\gamma\left(\alpha - \rho v^2\right)}}{2\gamma}, \tag{4.50}$$

and $b \to 0$ in the high wave number limit. Using eqn (2.7) with eqn (4.49) gives the analogous form of eqns (4.39) and (4.40), namely

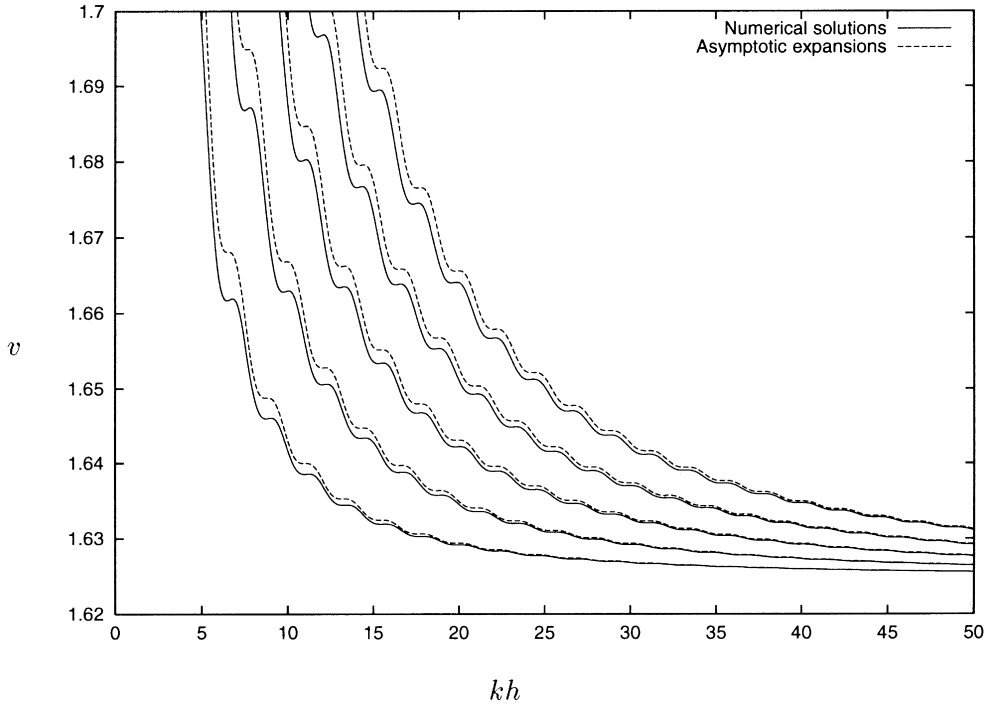

Fig. 7. Comparison of numerical solutions with asymptotic expansions obtained for Case 3, see eqn (4.48). The same material parameters from Fig. 3 are used

$$a = a_0 + a_1 b^2 + O(b^4), \tag{4.51}$$

where

$$a_0 = -1 + \gamma^{1/2}(\alpha + \gamma - 2\beta)^{1/2}, \quad a_1 = \frac{1}{2(a_0 + 1)}. \tag{4.52}$$

On making use of the expansions shown in eqns (4.49) and (4.51) it is deduced that for high wave number eqn (2.12) takes the form

$$\begin{aligned} &4\hat{q}_1\hat{q}_2 f(q_1) f(q_2)\Delta_1 + \left\{\hat{q}_1 f(q_2)^2 - \hat{q}_2 f(q_1)^2\right\} \\ &\quad \times \left\{(\Delta_5 - \Delta_2)\sin\left\{2\left(\sqrt{a_0} + \xi b^2\right)kh\right\} + (\Delta_3 + \Delta_4)\cos\left\{2\left(\sqrt{a_0} + \xi b^2\right)kh\right\}\right\} \\ &\quad = \left\{\hat{q}_1 f(q_2)^2 + \hat{q}_2 f(q_1)^2\right\}\left\{(\Delta_2 + \Delta_5)S(b) + (\Delta_4 - \Delta_3)C(b)\right\} + O(b^3), \end{aligned} \tag{4.53}$$

within which $\hat{q}_1$ and $\hat{q}_2$ are approximated by

$$\begin{aligned} \hat{q}_1 &= \sqrt{a_0} - \frac{b}{2\sqrt{a_0}} + \xi b^2 + O(b^3), \\ \hat{q}_2 &= \sqrt{a_0} + \frac{b}{2\sqrt{a_0}} + \xi b^2 + O(b^3), \end{aligned} \tag{4.54}$$

and $\xi = (4a_0a_1 - 1)/8a_0^{3/2}$. It will be seen subsequently that the leading-order term of eqn (4.53) vanishes

in the limit, thus necessitating the inclusion of $O(b^2)$ terms in all expansions of the components of the dispersion relation. From eqns $(4.50)_1$ and (4.51) we have

$$\rho v^2 = 2\beta + 2\gamma\left(a_0 + a_1 b^2\right) + O(b^4). \tag{4.55}$$

On inserting eqn (4.55) into the appropriate form of eqn (2.6), and after a little algebraic manipulation, expansions for p_1 and p_2 are obtained, namely

$$p_1 = p_1^{(0)} + p_1^{(2)} b^2 + O(b^4), \quad p_2 = p_2^{(0)} + p_2^{(2)} b^2 + O(b^4), \tag{4.56}$$

where

$$p_1^{(0)} = \left(\frac{\lambda_0 + \mu_0}{2\tilde{\gamma}}\right)^{1/2}, \quad p_1^{(2)} = \frac{\mu_2/2\mu_0 - 2\gamma a_1 \tilde{\rho}/\rho}{2\left(2\tilde{\gamma}\right)^{1/2}\left(\lambda_0 + \mu_0\right)^{1/2}},$$

$$p_2^{(0)} = \left(\frac{\lambda_0 - \mu_0}{2\tilde{\gamma}}\right)^{1/2}, \quad p_2^{(2)} = -\frac{\mu_2/2\mu_0 + 2\gamma a_1 \tilde{\rho}/\rho}{2\left(2\tilde{\gamma}\right)^{1/2}\left(\lambda_0 - \mu_0\right)^{1/2}},$$

and within which

$$\lambda_0 = 2\tilde{\beta} - \frac{\tilde{\rho}}{\rho}(2\beta + 2\gamma a_0),$$

$$\mu_0 = \left\{4\left(\tilde{\beta}^2 - \tilde{\alpha}\tilde{\gamma}\right) + \left(2\tilde{\beta} - \lambda_0\right)^2 + 4\left(\tilde{\gamma} - \tilde{\beta}\right)\left(2\tilde{\beta} - \lambda_0\right)\right\}^{1/2},$$

$$\mu_2 = 4\frac{\tilde{\rho}}{\rho}\gamma a_1\left(2\tilde{\gamma} - \lambda_0\right).$$

Similar expansions for $f(q)$ and $\tilde{f}(p)$ are obtainable by making use of eqns (4.54) and (4.56), namely

$$f(q_1), f(q_2) = f^{(0)} \pm f^{(1)} b + f^{(2)} b^2 + O(b^3),$$
$$\tilde{f}(p_1) = \tilde{f}_1^{(0)} + \tilde{f}_1^{(2)} b^2 + O(b^4), \quad \tilde{f}(p_2) = \tilde{f}_2^{(0)} + \tilde{f}_2^{(2)} b^2 + O(b^4), \tag{4.57}$$

where

$$f^{(0)} = \gamma(1 - a_0) - \sigma_2, \quad f^{(1)} = \gamma, \quad f^{(2)} = -\gamma a_1,$$

$$\tilde{f}_1^{(0)} = \tilde{\gamma} + \frac{\lambda_0 + \mu_0}{2} - \sigma_2, \quad \tilde{f}_1^{(2)} = \frac{\mu_2}{4\mu_0} - \gamma a_1 \frac{\tilde{\rho}}{\rho},$$

$$\tilde{f}_2^{(0)} = \tilde{\gamma} + \frac{\lambda_0 - \mu_0}{2} - \sigma_2, \quad \tilde{f}_2^{(2)} = -\frac{\mu_2}{4\mu_0} - \gamma a_1 \frac{\tilde{\rho}}{\rho}.$$

Using eqns (4.54), (4.56) and (4.57), in conjunction with eqn (4.53) the dispersion relation in the high wave number region may be cast in the form

$$\mathscr{A}_1 + \left(\mathscr{A}_2 - \mathscr{A}_3 C(a_0) - \mathscr{A}_4 S(a_0)\right) b^2 = \left(\mathscr{A}_1 + \mathscr{A}_5 b^2\right) C(b) + \mathscr{A}_6 b S(b) + O(b^3), \tag{4.58}$$

where $C(a_0)$, $S(a_0)$, $C(b)$ and $S(b)$ are trigonometric terms which may be inferred from the definitions given directly after eqn (4.42), and $\mathscr{A}_m$ are order 1 quantities defined as

$$\mathscr{A}_1 = a_0\Delta_1^{(0)}f^{(0)^2},$$

$$\mathscr{A}_2 = \left(2\sqrt{a_0}\xi - \frac{1}{4a_0}\right)\Delta_1^{(0)}f^{(0)^2} + a_0\Delta_1^{(2)}f^{(0)^2} + a_0\Delta_1^{(0)}\left(2f^{(0)}f^{(2)} - f^{(1)^2}\right),$$

$$\mathscr{A}_3 = \left\{2\sqrt{a_0}f^{(0)}f^{(1)} + \frac{f^{(0)^2}}{2\sqrt{a_0}}\right\}\left\{\sqrt{a_0}\Delta_2^{(1)} - \frac{\Delta_1^{(0)}}{2\sqrt{a_0}}\right\},$$

$$\mathscr{A}_4 = \left\{2\sqrt{a_0}f^{(0)}f^{(1)} + \frac{f^{(0)^2}}{2\sqrt{a_0}}\right\}\left\{\left(p_1^{(0)}p_2^{(0)} - a_0\right)\left(\tilde{f}_1^{(0)} - \tilde{f}_2^{(0)}\right)f^{(1)}\right\},$$

$$\mathscr{A}_5 = 2\sqrt{a_0}\Delta_1^{(0)}f^{(0)^2}\xi - a_0\Delta_2^{(2)}f^{(0)^2} - \frac{\Delta_3^{(1)}f^{(0)^2}}{2}$$
$$+\Delta_1^{(0)}\left\{a_0f^{(1)^2} + 2a_0f^{(0)}f^{(1)} + f^{(0)}f^{(1)}\right\},$$

$$\mathscr{A}_6 = \sqrt{a_0}f^{(0)^2}f^{(1)}\left(a_0 + p_1^{(0)}p_2^{(0)}\right)\left(\tilde{f}_2^{(0)} - \tilde{f}_1^{(0)}\right). \tag{4.59}$$

Within eqn (4.59) $\Delta_i^{(m)}$ represents the coefficients of b^m in Δ_i, which may be obtained by inserting the expansions given in eqns (4.54), (4.56) and (4.57) into eqn (2.13), dividing throughout by $C_1\,C_2\,\tilde{C}_1\,\tilde{C}_2$, and replacing the resulting hyperbolic tangents with unity, thus

$$\Delta_1^{(0)} = p_2^{(0)}\left(f^{(0)} - \tilde{f}_1^{(0)}\right)^2 - p_1^{(0)}\left(f^{(0)} - \tilde{f}_2^{(0)}\right)^2,$$

$$\Delta_1^{(2)} = 2p_1^{(0)}\left(f^{(0)} - \tilde{f}_2^{(0)}\right)\left(\tilde{f}_2^{(2)} - f^{(2)}\right) + 2p_2^{(0)}\left(f^{(0)} - \tilde{f}_1^{(0)}\right)\left(f^{(2)} - \tilde{f}_1^{(2)}\right)$$
$$+f^{(1)^2}\left(p_1^{(0)} - p_2^{(0)}\right) + p_2^{(2)}\left(f^{(0)} - \tilde{f}_1^{(0)}\right)^2 - p_1^{(2)}\left(f^{(0)} - \tilde{f}_2^{(2)}\right)^2,$$

$$\Delta_2^{(1)} = 2f^{(1)}\left\{p_1^{(0)}\left(f^{(0)} - \tilde{f}_2^{(0)}\right) - p_2^{(0)}\left(f^{(0)} - \tilde{f}_1^{(0)}\right)\right\},$$

$$\Delta_2^{(2)} = 2f^{(1)^2}\left(p_1^{(0)} - p_2^{(0)}\right) - \Delta_1^{(2)}. \tag{4.60}$$

It is readily deduced from eqn (4.58) that to leading order

$$\left(1 - \cos\frac{bkh}{\sqrt{a_0}}\right) \sim O(b)\sin\frac{bkh}{\sqrt{a_0}}, \tag{4.61}$$

thus implying that $\cos(bkh/\sqrt{a_0}) \to 1$ as $kh, kd \to \infty$ and therefore,

$$b = 2\sqrt{a_0}\,\frac{n\pi}{kh} + O(kh)^{-2}. \tag{4.62}$$

A second-order approximation to the phase speed may be found by inserting eqn (4.62) into eqn (4.55), to obtain

$$\rho v_n^2 = 2\beta - 2\gamma + 2\gamma^{1/2}(\alpha + \gamma - 2\beta)^{1/2} + \left\{\frac{\gamma a_0}{a_0 + 1}\right\}\left(\frac{n\pi}{kh}\right)^2 + \cdots. \tag{4.63}$$

We then seek a higher-order expansion by setting

$$b = 2\sqrt{a_0}\,\frac{n\pi}{kh} + \frac{\phi_4}{(kh)^2} + O(kh)^{-3} \tag{4.64}$$

from which it is deduced that

$$\sin\left(\frac{bkh}{\sqrt{a_0}}\right) = \frac{\phi_4}{\sqrt{a_0}kh} + O(kh)^{-3}, \quad \cos\left(\frac{bkh}{\sqrt{a_0}}\right) = 1 - \frac{\phi_4^2}{2a_0(kh)^2} + O(kh)^{-4}, \tag{4.65}$$

where ϕ_4 is to be determined and it is noted that it is now necessary to include an $O(kh)^{-2}$ term in the expansion $(4.65)_2$ due to the vanishing of the leading order term prior to the derivation of eqn (4.58). Inserting eqns (4.64) and (4.65) into eqn (4.58) and comparing like powers of kh reveals that the equation is identically zero at leading order, the next order yielding the following quadratic equation for ϕ_4

$$\frac{\mathscr{A}_1}{2a_0}\phi_4^2 - 2\mathscr{A}_6 n\pi\phi_4 + 4a_0 n^2\pi^2\{\mathscr{A}_2 - \mathscr{A}_5 - \mathscr{A}_3 C(a_0) - \mathscr{A}_4 S(a_0)\} = 0. \tag{4.66}$$

It is interesting to note that in this case a quadratic equation for ϕ_4 is obtained, whilst in the previous three cases a single value for ϕ_1, ϕ_2 and ϕ_3 was obtained. However, it has been verified numerically that for particular values of n the two solutions indicated in eqn (4.66) correspond to two distinct branches of the dispersion relation. This is, perhaps, not too surprising as we have seen in Fig. 4 that the harmonics group together to form distinct pairs in the high wave number region. Indeed the second-order approximation to the phase speed in eqn (4.63) gives asymptotic solutions which pass between adjacent pairs of harmonics, thus in order to obtain accurate asymptotic solutions the expansion must be taken to at least third-order. Moreover in the first two cases a reasonable approximation may be found from the second-order expansion and although the second-order expansion in the third case cannot describe the oscillatory behaviour at least an approximation for each harmonics is obtained. Eqn (4.66) may therefore be used, in conjunction with eqns (4.64) and (4.50)), to obtain

$$\rho v_n^2 = \begin{cases} \rho v_{S_2}^2 + \left(\dfrac{n+1}{2}\right)^2 \left(\dfrac{\pi}{kh}\right)^2 \left\{\dfrac{4\gamma}{a_0+1}\right\}\left\{a_0 + \dfrac{\sqrt{a_0}\hat{\phi}_4^-}{kh}\right\} + \cdots & n \text{ odd} \\ \rho v_{S_2}^2 + \left(\dfrac{n\pi}{2kh}\right)^2 \left\{\dfrac{4\gamma}{a_0+1}\right\}\left\{a_0 + \dfrac{\sqrt{a_0}\hat{\phi}_4^+}{kh}\right\} + \cdots & n \text{ even} \end{cases}, \tag{4.67}$$

$\hat{\phi}_4 = \phi_4/n\pi$, ϕ_4^+ and ϕ_4^- representing solutions of eqn (4.66), indicating the positive and negative square root associated with the discriminant, respectively. It is worth noting that the asymptotic expansions indicated in eqn (4.67) also arise in the analogous flexural wave expansions, see Rogerson and Sandiford (1997, eqn (4.68)). This arises for the same reason as that given in Case 1.

The asymptotic expansions obtained in eqn (4.67) are superimposed upon numerical solutions in Fig. 8. The material parameters used have been taken from Fig. 4. The asymptotic expansions again give good agreement with the numerical solutions and describe the oscillatory behaviour of the harmonics in the moderate and high wave number regions.

5. Surface wave-like behaviour of the higher harmonics

The possibility of surface wave-like behaviour arising from the combined contribution of higher harmonics has been indicated from the numerical results obtained in Fig. 2. Such a possibility will arise

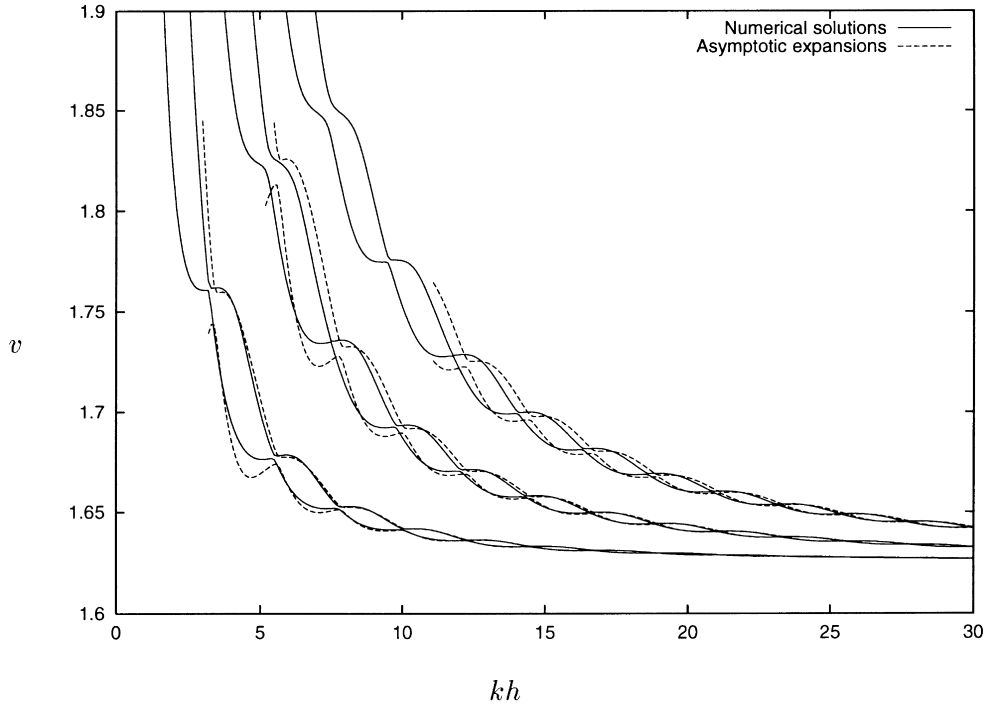

Fig. 8. Comparison of numerical solutions with asymptotic expansions obtained for Case 4, see eqn (4.67). The same material parameters from Fig. 4 are used.

when the high wave number limit of the harmonics is associated with the inner core and a real value of the surface wave speed exists such that $v_R > \tilde{v}_L$. This is investigated further here by examining the eigenfunctions U and V as the wave speed of a particular harmonic in such a situation passes through the surface wave speed value. For any root of the dispersion relation it is possible to use the homogeneous boundary and continuity conditions to obtain expressions for U and V in terms of an arbitrary costant. From these solutions, the variation of displacement throughout the laminate may be obtained.

Fig. 9 and 10 show the normalised in-plane ($\hat{U}$) and out-plane ($\hat{V}$) displacements associated with the fourth harmonic of Fig. 2 as it passes through the surface wave speed value at various values of scaled wave number. The width of the laminate has been scaled so that the upper and lower surfaces are at $x_2 = \pm 2$ and the interfaces are at $x_2 = \pm 1$, thus representing all cases in which the ratio of ply thickness is such $d/h = 1$. Four values of scaled wave number have been chosen in order to show the behaviour of the in-plane and out-plane displacements. Due to the extremely sharp flattening of the dispersion curves around v_R in Fig. 2, the increment between successive values of kh is small. For the first value used, $kh = 12.080$, there is no clear localisation of displacement at any point within the laminate, with the displacement at each surface small in relation to that in the inner core. The nature of the displacement is clearly sinusoidal. When the wave number is increased slightly to $kh = 12.083$, the graph changes significantly, in that the displacement is clearly localised at each surface, with only small sinusoidal variation in the inner core. This sinusoidal variation decreases further as the wave number is increased to $kh = 12.085$. The displacement in the outer layers ($x_2 \leqslant -1$ and $x_2 \geqslant 1$) is indistinguishable

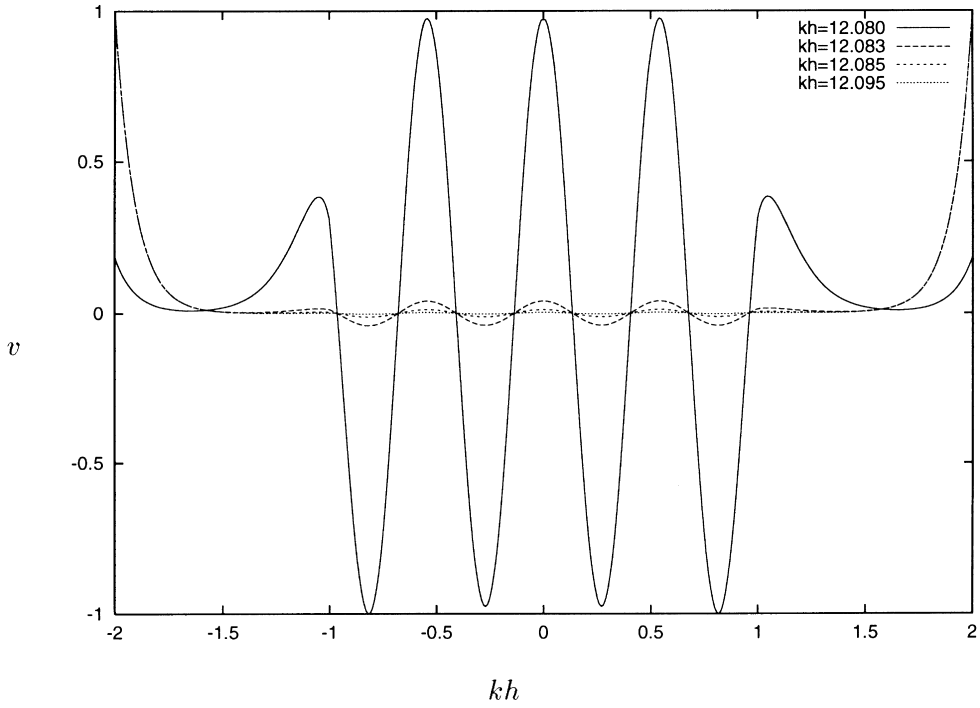

Fig. 9. Scaled eigenfunction $\hat{U}$ against depth of the laminate for the fourth harmonic of Fig. 2, showing the change from sinusoidal displacement to surface wave-like behaviour as the phase speed passes through v_R.

from that obtained using the previous value of kh, with the associated curves overlapping in this region. The final value of kh exhibits classic surface wave behaviour, with strong localisation of displacement at each free surface and no discernible displacement in the inner core. This suggests that a surface wave front will indeed be formed from the combined effects of the harmonics as they pass through the value of v_R. In addition, the nature of the displacement associated with a particular harmonic can change dramatically for small changes in the wave number (e.g. as small as 0.003 in Figs. 9 and 10). It is worth noting that for the four values of kh used here the wave speed in each case varies only at the fifth decimal place.

6. Comparison of flexural and extensional wave results

This paper is concluded with a short section presenting some closing remarks on the results obtained numerically and analytically for the two dispersion relations associated with flexural and extensional waves. The close similarity of the two dispersion relations, as is to be expected, gives rise to similar solutions which differ in small but significant ways. A cursory comparison of the extensional dispersion relation (2.12) with the appropriate flexural dispersion relation, see Rogerson and Sandiford (1997, eqn (3.18)), reveals that they only differ in a subtle permutation of the hyperbolic terms associated with the inner core, namely that $\tilde{C}_m \leftrightarrow \tilde{S}_m$. This has the effect that the two dispersion relations will act identically in the high wave regime when p_1 and p_2 are real or complex conjugates (i.e. when the limiting behaviour of $\tanh kp_m d$ is well defined). This situation arises in the asymptotic expansions for the high

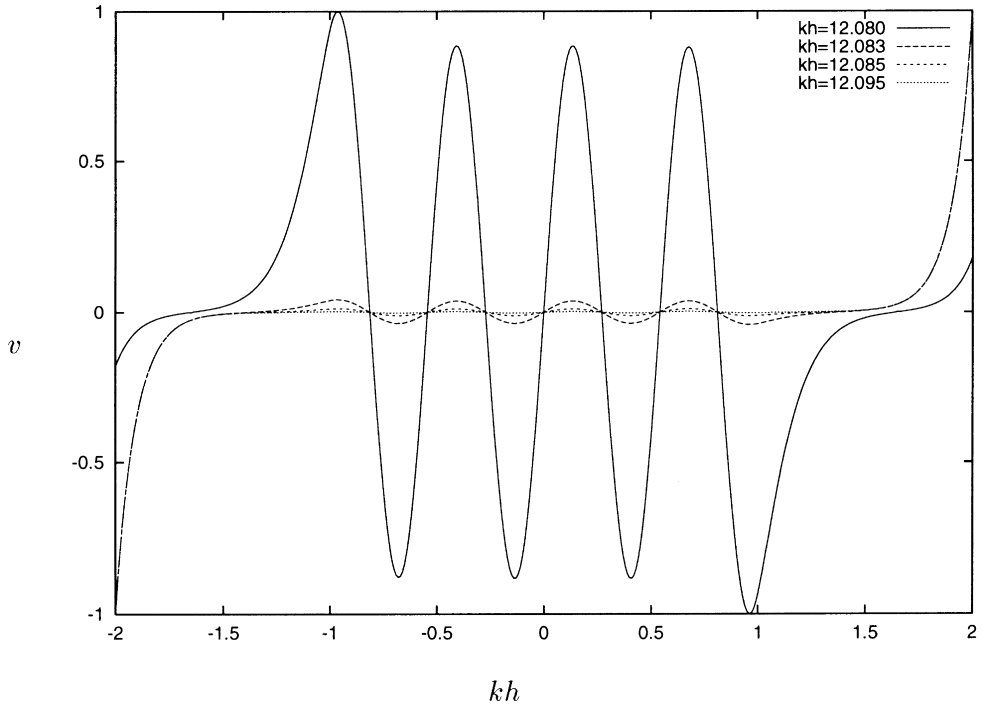

Fig. 10. Scaled eigenfunction $\hat{V}$ against depth of the laminate for the fourth harmonic of Fig. 2, showing the change from sinusoidal displacement to surface wave-like behaviour as the phase speed passes through v_R.

wave number limit of the dispersion relations in Cases 1 and 4 ($v \to v_{S_1}$ and $v \to v_{S_2}$). Conversely, one should expect the two dispersion relations to behave differently when this is not the case. This is examined in Figs. 11–14, which present plots of the numerical solutions for both flexural and extensional waves superimposed upon one another for each of the four cases outlined in the asymptotic expansions for the high wave limit.

The dispersion curves for Case 1 ($v \to v_{S_1}$) are shown in Fig. 11, and are generated using the material parameters from Fig. 1. The first fifteen branches from each of the flexural and extensional modes are shown. It appears that in this case the flexural and extensional modes merge together below a certain value of the phase speed. This behaviour differs significantly than that observed for a single layer plate in the same limit ($v \to v_{S_1}$), in which the flexural and extensional modes interlace and do not coalesce, see Rogerson (1997). For high kh this threshold value corresponds to the shear wave speed in the inner core, $\tilde{v}_{S_1} = 2.0$. Below this value p_1 and p_2 take on real values and hence, as the limiting behaviour of $\tanh kp_m d$ is well defined, the two dispersion relations behave similarly. Above the threshold value one of p_1 and p_2 is imaginary, the other real, and the difference in the two dispersion relations between flexural and extensional modes plays a significant part due to the existence of trigonometrical terms.

Fig. 12 shows numerical solutions for Case 2 ($v \to \tilde{v}_{S_1}$) generated using the parameters in Fig. 2. The first fifteen branches from each figure are used. From the figure it is clear that the flexural and extensional modes alternate, with the fundamental mode from the flexural solutions having lowest wave speed. This situation mirrors the behaviour of flexural and extensional modes in the single plate problem, see Rogerson (1997). Only the fundamental modes retain finite wave speed as $kh \to 0$ and all harmonics asymptote to the shear wave speed v_{S_1}.

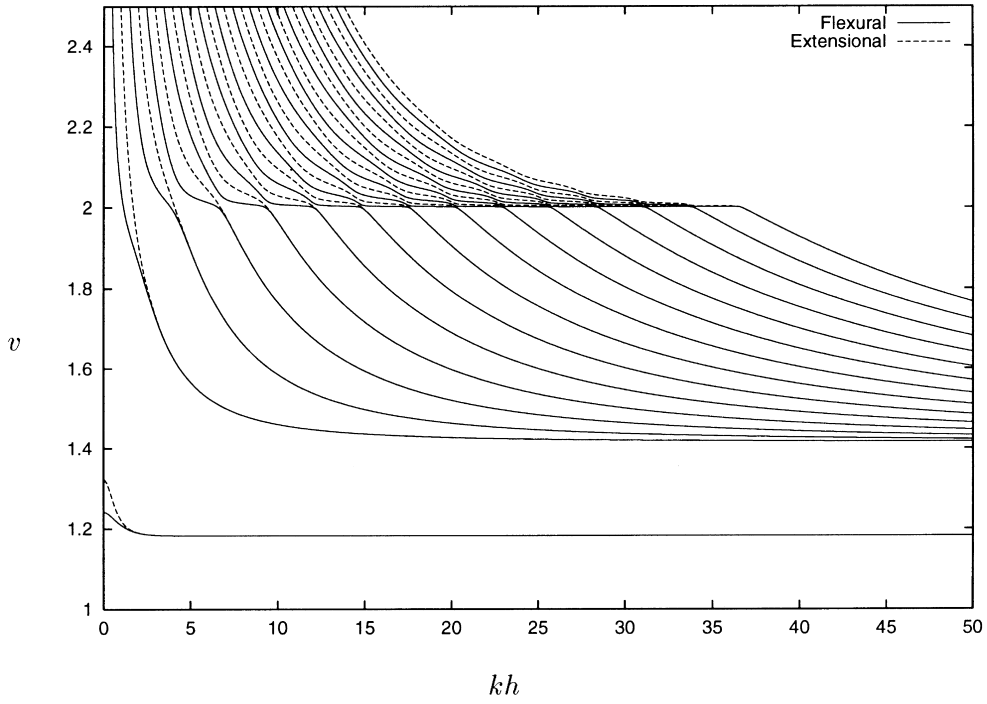

Fig. 11. Comparison of flexural and extensional solutions for Case 1: $v \to v_{S_1}$.

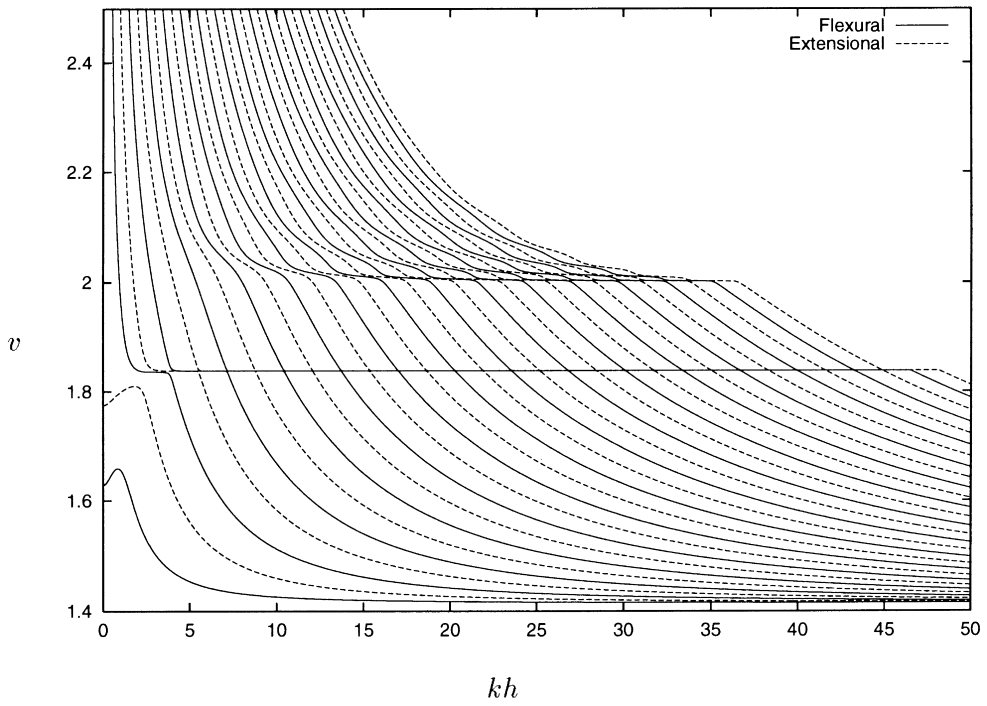

Fig. 12. Comparison of flexural and extensional solutions for Case 2: $v \to \bar{v}_{S_1}$.

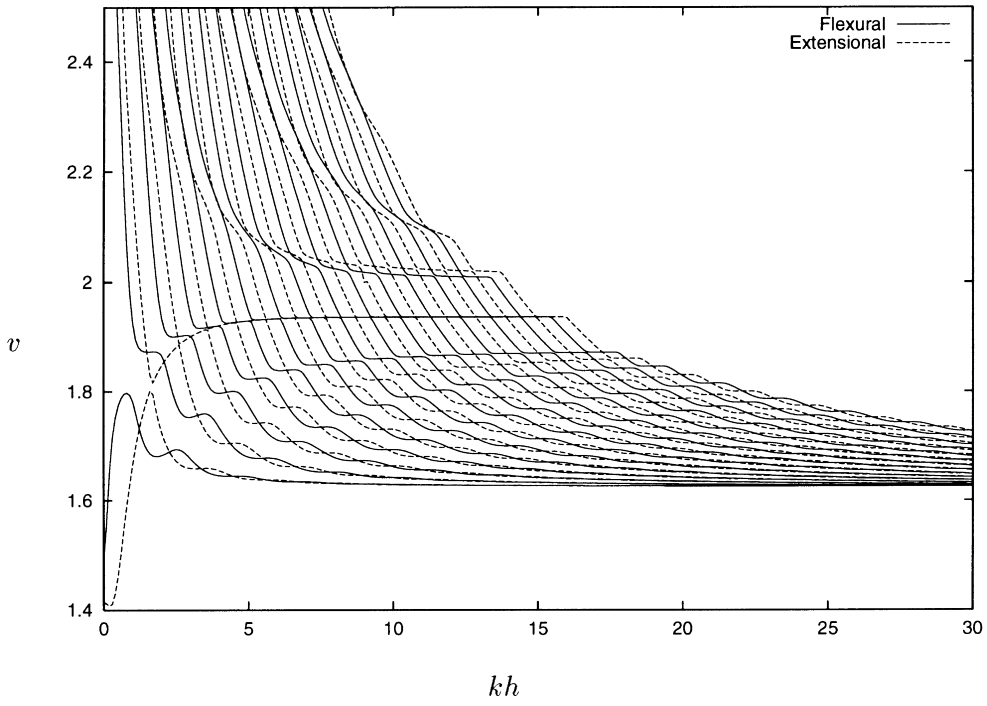

Fig. 13. Comparison of flexural and extensional solutions for Case 3: $v \to \bar{v}_{S_2}$.

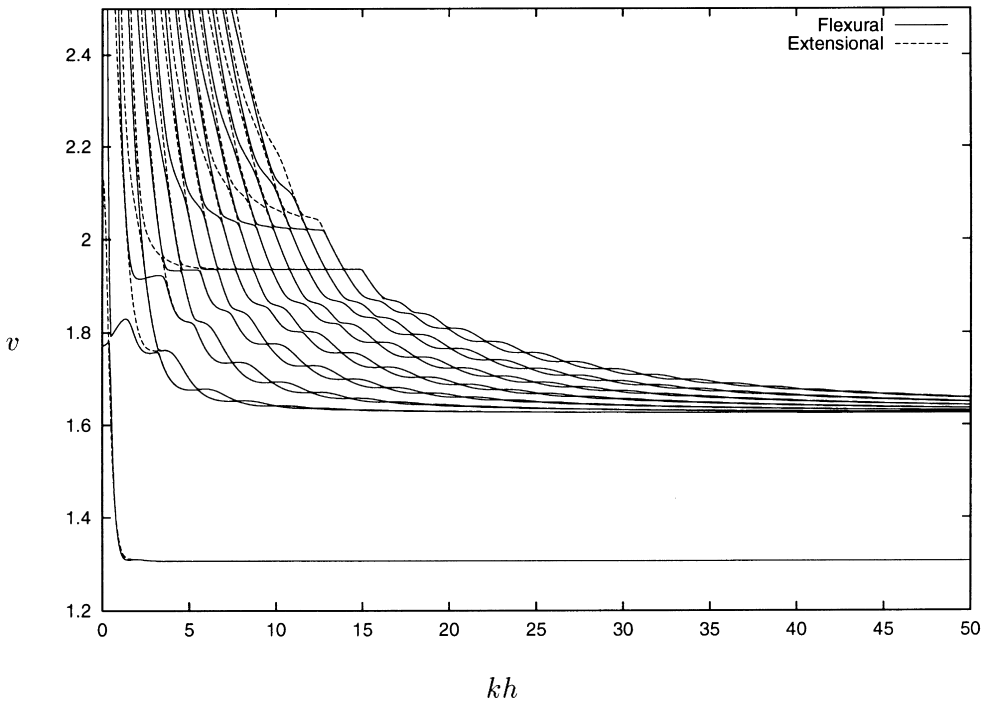

Fig. 14. Comparison of flexural and extensional solutions for Case 4: $v \to v_{S_2}$.

Case 3, $v \to \tilde{v}_{S_2}$ is presented in the next plot. Fig. 13 shows the first fifteen branches of the flexural and extensional dispersion relations generated from the parameters used in Fig. 3. The behaviour of the flexural and extensional modes is similar to that in Fig. 11 for phase speed greater than $\tilde{v}_{S_1} = 1.876$, in that the flexural and extensional modes alternate. However, below this value of the phase speed, while the mode still alternate, it is evident that the extensional and flexural modes associated with a particular harmonic number cross each other due to the sinusoidal variation. It is interesting to note that for each of the ghost lines associated with the shear wave speeds v_{S_1} and $\tilde{v}_{S_1}$ the harmonics associated with the flexural solutions asymptote to the appropriate value quicker than the extensional harmonics.

The final case ($v \to \tilde{v}_{S_2}$) is compared in Fig. 14, which is generated from the material parameters used in Fig. 4. The behaviour of the two dispersion curves for flexural and extensional waves is more complicated in this case. For phase speeds higher than $v = v_{S_1}$ ($= 2.012$) the flexural and extensional modes alternate. Below this value the branches associated with flexural and extensional modes begin to coalesce, with all branches having done so at a low wave number. This is to be expected as within this region p_1 and p_2 take on complex conjugate values below $v = 2.012$ and thus the difference between the dispersion relations is negligible for high wave number.

Appendix

For the distance $x_2 - \tilde{x} = h$, say, the components of the propagator matrix $\mathbf{P}(h)$ are given by

$$P_{11} = q_1 q_2 \{f(q_2)C_2 - f(q_1)C_1\}\mu^{-1}, \quad P_{12} = q_1 q_2 \{q_1 f(q_2)S_1 - q_2 f(q_1)S_2\}\mu^{-1},$$

$$P_{13} = q_1 q_2 \{q_2 S_2 - q_1 S_1\}\mu^{-1}, \quad P_{14} = q_1 q_2 \{C_1 - C_2\}\mu^{-1},$$

$$P_{21} = \{q_1 f(q_2)S_2 - q_2 f(q_1)S_1\}\mu^{-1}, \quad P_{22} = q_1 q_2 \{f(q_2)C_1 - f(q_1)C_2\}\mu^{-1},$$

$$P_{23} = -P_{14}, \quad P_{24} = \{q_2 S_1 - q_1 S_2\}\mu^{-1},$$

$$P_{31} = \left\{q_1 f(q_2)^2 S_2 - q_2 f(q_1)^2 S_1\right\}\mu^{-1}, \quad P_{32} = q_1 q_2 f(q_1) f(q_2)\{C_1 - C_2\}\mu^{-1},$$

$$P_{33} = P_{11}, \quad P_{34} = \{q_2 f(q_1)S_1 - q_1 f(q_2)S_2\}\mu^{-1},$$

$$P_{41} = q_1 q_2 f(q_1) f(q_2)\{C_2 - C_1\}\mu^{-1}, \quad P_{42} = q_1 q_2 \left\{q_1 f(q_2)^2 S_1 - q_2 f(q_1)^2 S_2\right\}\mu^{-1},$$

$$P_{43} = q_1 q_2 \{q_2 f(q_1)S_2 - q_1 f(q_2)S_1\}\mu^{-1}, \quad P_{44} = P_{22},$$

where $S_m = \sinh(kq_m h)$ and $C_m = \cosh(kq_m h)$.

References

Dowaikh, M.A., Ogden, R.W., 1990. On surface waves and deformations in a pre-stressed incompressible elastic solid. IMA J. of Appl. Math. 44, 261–284.

Dowaikh, M.A., Ogden, R.W., 1991. Interfacial waves and deformations in pre-stressed elastic media. Proc. R. Soc. Lond. A. 433, 313–328.

Flavin, J.N., 1963. Surface waves in pre-stressed Mooney material. Q. J. Mech. Appl. Mech. 16, 441–449.

Gilbert, F., Backus, G.E., 1966. Propagator matrices in elastic wave and vibration problems. Geophysics 31, 326–332.

Hayes, M.A., Rivlin, R.S., 1961. Surface waves in deformed elastic materials. Arch. Ration. Mech. Anal. 8, 358–380.

Ogden, R.W., Roxburgh, D.G., 1993. The effect of pre-stress on the vibration and stability of elastic plates. Int. J. Eng. Sci. 30, 1611–1639.

Rogerson, G.A., 1997. Some asymptotic expansions of the dispersion relation for an incompressible elastic plate. Int. J. Solids Structures 34 (22), 2785–2802.

Rogerson, G.A., Fu, Y.B., 1995. An asymptotic analysis of the dispersion relation of a pre-stressed incompressible elastic plate. Acta Mechanica 111, 59–77.

Rogerson, G.A., Sandiford, K.J., 1996. On small amplitude vibrations of pre-stresses laminates. Int. J. Eng. Sci. 34 (8), 853–872.

Rogerson, G.A., Sandiford, K.J., 1997. Flexural waves in incompressible pre-stressed elastic composites. Q. J. Mech. Appl. Math. 50 (4), 597–624.